Author comment on "Ten years of atmospheric methane from ground-based NDACC FTIR observations." by W. Bader et al.

We would like to thank the referees for their review and constructive comments. Please find below our responses to each comment.

Referee #1

General / Major Comments

The paper is concise restricting itself to 10 stations and 10 years of data but leaves a considerable amount of similar data out. There are more stations with archived data and many stations have data dating back to the mid 1990's and earlier. A description of this larger dataset would be considerably more illuminating and reflective of the longevity and efforts of the NDACC network. In a similar context of under reporting, Fig 3 proves stratospheric information is contained in these data yet these trends are not explored. Relative trends in the troposphere vs the stratosphere would be unique and important. It's not clear what advantage Fig 3 delivers when the information is ignored. Instead ACE-FTS date is invoked to discuss any stratospheric trend. While this data record is also long, it is sparse and not as long as the NDACC record.

We agree that the title may be misleading as to the premise of this paper. We would like to remind that the main objective of this paper is to discuss the recent increase of methane total columns and the possible cause(s) for this still unresolved upturn with the help of a GEOS-Chem tagged simulation, using a suite of sites covering a broad range of latitudes. Following Referee #1's comment and Referee #3's suggestions (see below), the title of this paper will be edited to "The recent increase of atmospheric methane from ten years of ground-based NDACC FTIR observations since 2005." In this framework, while we agree the NDACC data consists of an even largest dataset, the relative trends in the troposphere vs the stratosphere is beyond the scope of this paper.

Why was the CTM results stopped at 2013? This appears arbitrary and again leaves out information.

The time period studied for the GEOS-Chem simulation is due to the limited availability of the GEOS-5 meteorological fields. As mentioned in Page 8 Line 10 "The GEOS-Chem model output presented here covers the period January 2005-December 2012, for which the GEOS-5 meteorological fields are available." and in Page 9 Line 7 "Due to the availability of the GEOS-5 meteorological fields and to ensure consistency, we limited our comparison of methane changes between FTIR observations and the GEOS-Chem simulation over the 2005-2012 time period."

There is too little discussion of total uncertainty in the CH_4 columns. References to two other papers does not seem adequate in general and in particular given the use of noise in Wollongong data trends later in the paper as a reason for a mismatch in trend (Pg 9). Were errors even used in the trend analysis? If so were then nominal values or real i.e. derived from calculations for each measurement?

The bootstrap method used for the trend analysis (Gardiner et al., 2008) accounts for the distribution of the data and by using the residual deviations of a model fit to the data as a representation of the random effects reflected in the data. Through an iterative process (repeated n time, n=5000 in this paper), those residual deviations are included in a new model fit in order to provide a good approximation to the distribution for the trend results. The 2.5 and 97.5 percentiles of this empirical distribution specify a 95% confidence interval associated with the annual change. This 95% confidence interval is mentioned in former Table 3 (now Table 2, see below).

Pg 6 Is a discussion of a type of normalization process with a stated purpose "to characterize the possible impact of the choice of the microwindows and spectroscopy on the retrieved methane". A set of data from JFJ is fit by all other stations using their local method and hence a relative station bias to Jungfraujoch is determined and consequently applied to each respective dataset.

The manuscript does not mention any normalization nor correction of each FTIR observations in any way (except for the Toronto retrievals during from 2008 to early 2009). The anomaly mentioned in the paper is computed for displaying purposes, in order for the reader to focus on the observed increase independently from absolute methane total column values which varies from one station to another.

1. This does not "characterize" effects of retrieval parameters. There is no further discussion to investigate this issue i.e. there is no actual characterization. There may be valid reasons to use differing parameters at different sites (e.g. interfering species) that may have unintended consequences when fitting JFJ spectra. A characterization exercise might reveal this.
2. The station bias values are not given, only a mean, this further obscures any understanding of the bias. These should at least be listed in Table 2 or 3.

In this paper, we use the optimized retrieval strategies currently available. The ideal way of thoroughly characterizing the effects of the retrieval parameters would be to perform an Observation System Simulation Experiment (OSSE) which is beyond the scope of this paper.

Following the reviewer's comment, Page 5, Line 26 has been edited:

> "In order to investigate ~~characterize~~ on the possible impact of the choice of the microwindows and spectroscopy on the retrieved methane, each strategy has been tested over a set of spectra recorded at the Jungfraujoch station (3068 spectra recorded between 01-01-2005 and 12-31-2012)."

We want to emphasize on how the choice of retrieval strategy has statistically no impact on the computed trends. In addition to the tests performed on a subset of Jungfraujoch observations, a similar exercise has been performed for Lauder observations. Changes of methane in Lauder from the strategy as described in (Sussmann et al., 2011) amounts at 0.28 ± 0.03 %/year which is in agreement with the value of 0.31 ± 0.03 %/year reported in this work. We can therefore conclude that the choice of the retrieval strategy has a marginal impact on methane changes even for wet sites.

3. Within the NDACC, these types of retrieval parameters are clearly defined yet many stations apparently do no use them (Table 2) this seems counterproductive to the goals of the network.

Among the official NDACC targets, methane is an exception (see also below), only because improved line parameters are needed in order to fully harmonize the approaches and exploit the spectra. For the other gases, the harmonization is in very good shape, and this comment does not hold true. We would also like to stress that despite this, the systematic bias resulting from the use of slightly different retrieval strategies has only a marginal effect on the total columns, and no effect on the trends.

4. Also if the retrievals are not performed to the NDACC standard are they indeed NDACC data? Are these data (meaning the 10y dataset from each station) found on the NDACC Archive? Or are they a separate retrieval? If they are not on the archive then they are not NDACC data and the premise of the manuscript is not at least completely valid.

While the harmonization of the retrieval strategy for methane is still a work under progress (as improved linelist parameters for methane are still required), it is worth mentioning that the retrieval strategies recommended by Sepúlveda et al. (2012) and Sussmann et al. (2011) share their main targeted CH_4 absorption lines and constraints. In order to be more comprehensive, Table 2 will be moved to an appendix (now Appendix A) where the limits of the windows and their corresponding interfering species will be mentioned, as well as the averaged DOFS for the time series studied.

The datasets presented here are the current optimized datasets for each station and 90% of them can be found on the NDACC Archive. While the archiving of the data is required for each NDACC site, this process is still under development for some station and mostly depend on funding and manpower availability.

The process to attain the anomaly plot Fig 5 is not described in sufficient detail. In particular the choice/method of terms in the annual cycles varying by site should be presented.

There is no adjustment of the seasonal cycle. We call here anomaly the time series expressed with respect to the value of the methane total column in 2005.0 as fitted by the Fourier series respective. For clarity, the equation for the computation of this anomaly is added in the article.

Page 5. Section 2.2.1. "Retrieval strategies"

> "The time series produced using the strategies described in Table 2 are illustrated in Fig. 2. In order to better illustrate the observed increase of methane total columns, t~~T~~he various panels show daily mean methane time series expressed as anomalies with respect to a reference column in 2005.0 (2006.0 for the Eureka station), according to the following equation :
>
> $$Anomaly = \frac{C-C_{05}}{(C+C_{05})\times 1/2}\times 100 \quad (1)$$
>
> where C is the methane total column and C_{05} the methane total column at the time 2005.0 derived from the linear component of the Fourier series (Gardiner et al., 2008) fitted to the time series ~~(see Sect. 3)~~."

Pg 13 top paragraph. 'No systematic bias' except of course, for possible biases removed earlier. This 3 station biases mentioned (Tsukuba, Lauder and Arrival Heights) – How are these determined?

Each bias has been computed with the same method, as mentioned Page 7 Line 27 : "Mean fractional differences are defined as the difference between two datasets divided by their arithmetic average and expressed in percent (see Eq. 2 in Strong et al., 2008)." The same reference has been added in this paragraph. The systematic biases identified between FTIR observations and the GEOS-Chem model have been added to now Table 2 (former Table 3).

Figure 5 is difficult to determine a comparison. Correlation plots would better illustrate the good agreement and bias of the two datasets. These should be replaced.

Figure 5 aims at providing a tool for comparison of methane increase since 2005 (and seasonal cycle) as observed and simulated rather than the bias between total column absolute value. In order to compare FTIR and GEOS-Chem methane total columns, the identified systematic biases have been added in Table 2 (former Table 3).

Minor issues

There were many issues with the model that could be explored. For instance, the seasonal amplitude in AH, Eureka & Kiruna. The inability to reproduce the variability at Toronto. There was mention of, but no explanation for the annual cycle phase difference at Izana & Tsukuba. There is a discussion of annual cycles and some mismatches (eg.JFJ, Izana). These are discussed only qualitatively when the data are available to quantify them. This would be an added benefit for the paper to put this in a table.

While we focused our analysis on comparisons of methane changes since 2005 between the observations and the simulation, quantification of the mismatched seasonal cycle for Tsukuba and Izaña are given in Page 9, Line 25. In order to better appraise the discrepancies or agreement between the FTIR observations and the GEOS-Chem model, the systematic bias between both time series has been added to Table 2 (former Table 3) for each station.

Its pointed out that the calculation of the trend at Wollongong could be effected by the early data variability. Could this early data not be removed from the trend calculation and compared as a shorter time series?

As the annual change of methane since 2005 is relatively small, it may easily be affected by noisier observations. However, it's worth mentioning that the best explanation for the discrepancies between FTIR and GEOS-Chem Wollongong methane is that sites such as Izaña or Wollongong "can be challenging sites for models to reproduce due to the topography and land-sea contrast (Kulawik et al., 2015)" (Page 10, Line 22). Removing the early data would only weaken the consistency of our methane changes analysis.

Pg 1 Ln 24 it appears misleading to state 'all members of the' The stations are all NDACC stations but not all NDAC station are used.

The sentence has been replaced by "Changes of atmospheric methane total columns (CH_4) since 2005 have been evaluated using Fourier Transform Infrared (FTIR) solar observations performed at ten ground-based sites affiliated to the Network for Detection of Atmospheric Composition Change (NDACC)."

Pg 1 Ln 36 'secondary contributors' is poorly defined simply minor might be a choice.
We don't think that "minor" is the best choice for non-negligible contributors amounting to 12-15% of the total, and we prefer to stick to the original expression.

Pg1 Ln 41 its not clear what the reference for 0.97 is.
The reference (Stocker et al., 2013) has been included.

Pg 2 Ln 9 – The statement 'significant uncertainties'. Is this in a statistical sense? Can these uncertainties actually be stated in the text especially given the discussion of attribution later in the text. Are they known?

This is not in a statistical sense as these uncertainties are unknown.
"and it is worth noting that these figures are still affected by significant uncertainties." will be replaced by "although it is worth noting that the global budget of methane remain insufficiently understood."

Pg 2 Ln 17 What is meant by "global surface climate change"?
Solomon et al. (2010) focuses on global surface climate change by estimating the contributions of stratospheric water vapor changes to the recent decadal rates of warming through analysis of correlation with the radiative forcing and sea surface temperature decadal changes.

Pg 3 Ln 25 Kiruna is not likely the most northern town in Sweden
Pg 4 – It may not be accurate to describe Toronto as a mega city.
Grammar, Spelling, Typographical issues
Pg 8 Ln 17 Fig 5.
Pg 17 Ln 30 shown
Pg 18 Ln 13 sources not tracers
The text will be modified accordingly.

Referee #2
General comments
In Page 5 line 15. The authors noted that CH_4 total columns for the Toronto site have a systematic error due to unknown instrument artifact and then made some manipulations with the data which seem to be doubtful. The main issue is how to separate (in data) the signals, which come from real atmospheric processes and from the instrument that doesn't work in a proper way. Could authors suggest more reasonable criteria/way for the correction of CH_4 time series for Toronto? Or, maybe, it would be better to omit Toronto site's data for the period of 2008-2009 from the analysis?

The time period associated to the instrument artifact of the Toronto data has been carefully identified based on observational logs. The constant offset used to correct this bias has been determined based on a method similar to the one used for the harmonization of two observational sets after a change in the instrumentation, for example. Find below the methane total column time series for Toronto in blue with the biased data displayed in red and the corrected data in green. While leading to the production of a consistent time series for methane observations above Toronto, this bias correction does not significantly impact the trend of methane which remains within the range of the averaged trend of 0.31 ± 0.03 for the 2005-2014 time period.

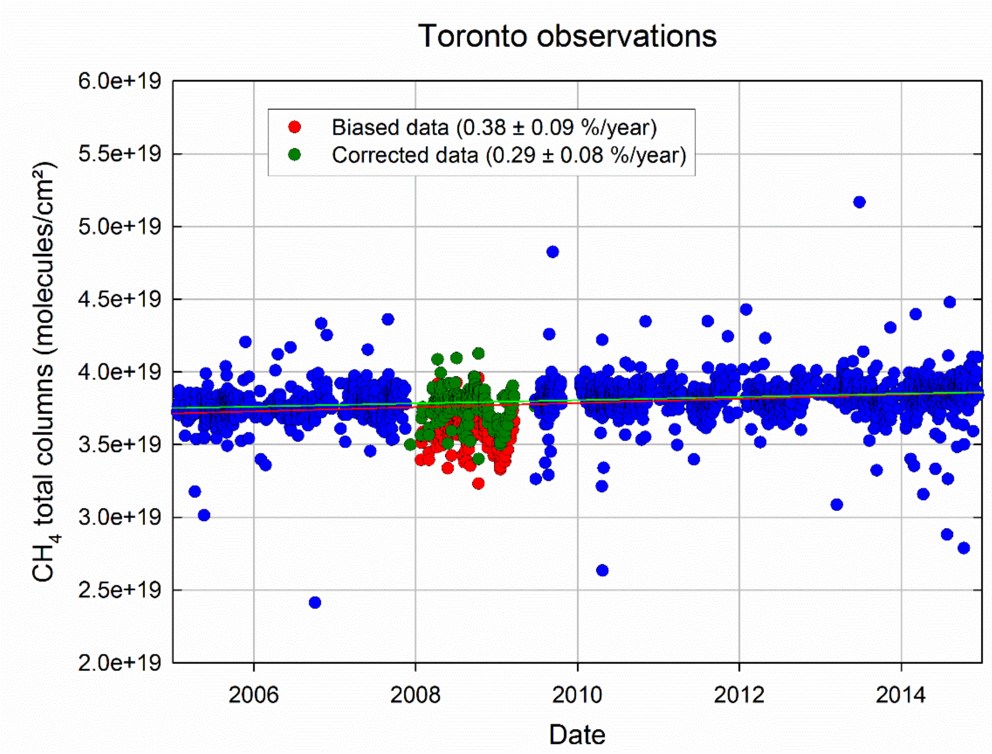

In Page 9 line 34. The explanation of the lower value of CH4 trend (0.22%/yr for 2005-2012) for the Jungfraujoch site given in the paper is in contradiction to the following: - according to a reference (Collaud Coen,2011), the coming of polluted air to the Jungfraujoch site was usually detected using the monitoring of CO, NOx and SO2 concentrations in the ambient air by local sensors. Authors need to bring compelling arguments proving that portions of polluted air, which can reach high altitude site, will significantly influence not only the concentrations of some gases but also the CH4 total column. - for Zugspitze (also a high altitude site), which is located not so far from Jungfraujoch, CH4 trend has the value of 0.31%/yr (2005-2012). Therefore it is worth to explain such noticeable difference between trends for Jungfraujoch and Zugspitze.

A various number of studies describe the Jungfraujoch observation site as a remote site (Henne et al., 2005, 2010; Okamoto and Tanimoto, 2016; Zellweger et al., 2000). Indeed, Ketterer et al., (2014) estimate the PBL height above Kleine Sheidegg (~5 km and 1.5 km horizontal and vertical distance from Jungfraujoch), with the help of remote sensing measurements of windprofiler signal to noise ratio and ceilometer aerosol backscattering profiles and show that influenced by PBL air masses transported upwards during summer. The study by Collaud Coen et al., (2011), through the in situ measurement of aerosol optic parameters, shows that PBL airmasses and its entire chemical and aerosol composition reaches JFJ height mostly during spring and summer as well. Moreover, as mentioned in Okamoto and Tanimoto, (2016), JFJ is exposed mostly to clean free tropospheric air masses in autumn and winter. In late spring and summer, it is intermittently influenced by vertically exported polluted air masses transported in the PBL over Europe (Zellweger et al., 2000, 2003).

On the other hand, Zugspitze has been classified by Henne et al., (2010) as a “weakly influenced, constant deposition” observation site. This difference between JFJ and ZUG while they are only 250 km apart and have a difference in altitude of 600 m can be explained by the more central Alpine location and higher elevation of Jungfraujoch (3580 m a.s.l.) compared to the position and elevation of Zugspitze (2954 m a.s.l.) at the northern flank of the Alps (see topography in the Figure below).

As to the GEOS-Chem model, the ZUG and JFJ simulations are extracted from two nearby pixels (see Figure below) where one is mostly flat (altitude of 781.8 m) and the other one montaneous (1352.1 m high). This explains the closeness of the results. Especially when what distinguishes both stations is mostly the influence of meteorological processes such as thermally driven transport (Forrer et al., 2000; Okamoto and Tanimoto, 2016) occurring at a local scale, which is still poorly represented by CTMs.

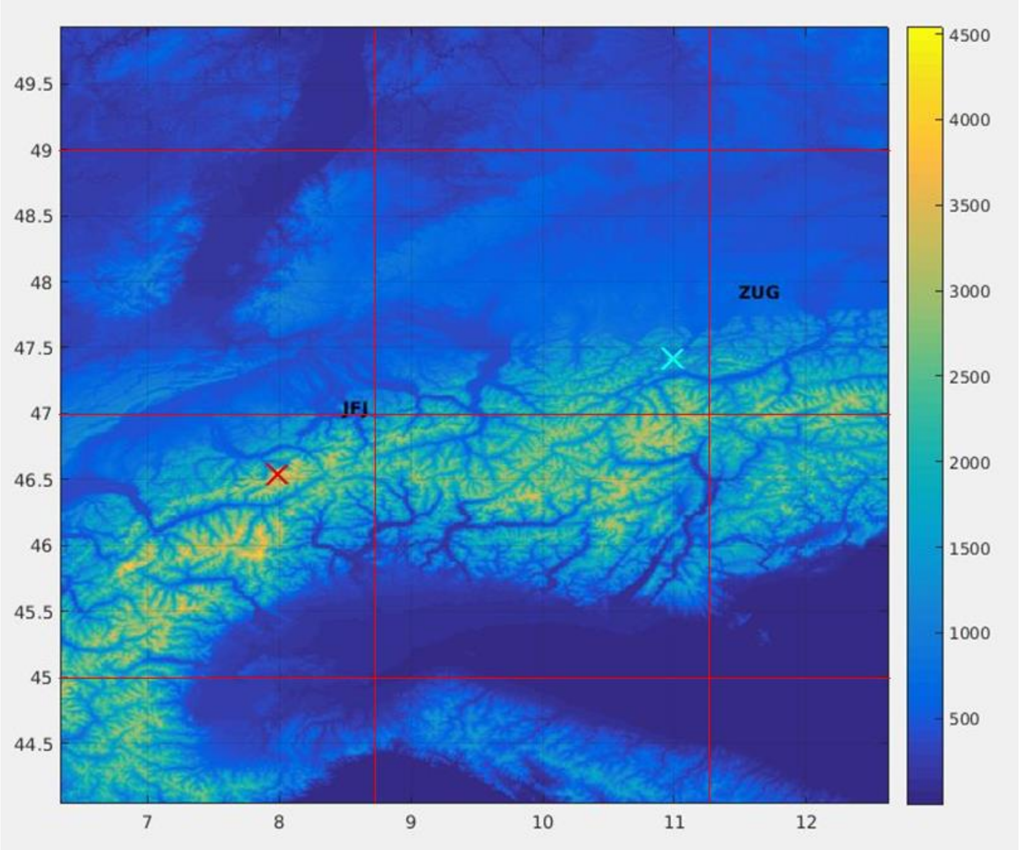

Alps topography with altitude (in meters). Red lines represent the GEOS-Chem 2°x2.5° horizontal grid, while red and cyan cross respectively show the Jungfraujoch and Zugspitze location.

From this comment, we would like to edit the mentioned paragraph as follows:

We first discuss the possible causes of the slight trend discrepancy between FTIR observations at Jungfraujoch and Zugspitze as well as with GEOS-Chem for both stations~~Jungfraujoch~~. Indeed, despite their proximity (~250 km apart) and their respective altitude of 3580 m and 2954 m, both Alpine sites show distinct influences from local thermal induced vertical transport. At mountain-~~-~~type sites, subsidence is predominant for anticyclonic weather conditions resulting in adiabatic warming and cloud dissipation. The clear sky and strong radiation conditions lead to the convective growth of the atmospheric boundary layer (ABL) that ~~and~~ induce thermal~~ly induced~~ injections of ABL air ~~can reach~~ to the high-altitude observation~~of those~~ sites (Collaud Coen et al., 2011; Henne et al., 2005; Nyeki et al., 2000). In addition, mountain venting induced by higher temperatures allows the transport of ABL air to the free troposphere occurring often in summer~~-~~(between April and Auguts; Henne et al., 2005; Kreipl, 2006)~~(between April and August; Henne et al., 2005)~~. While the~~At~~ Jungfraujoch site is a remote site mostly influenced by free tropospheric airmasses with incursions of ABL airmasses during 50% of the sping and summer time (Collaud Coen et al., 2011; Henne et al., 2005, 2010; Okamoto and Tanimoto, 2016; Zellweger et al., 2000, 2003), the Zugspitze site is more often influenced by the ABL (Henne et al., 2010). For summer, when the influence of the ABL is the largest, the observed changes are in very close agreement, with 0.25 ± 0.06 and 0.26 ± 0.09 %/year^{-1}, respectively. ~~the airmasses originating from the ABL amount to only 30% of the year (Collaud Coen et al., 2011). More specifically in summer, airmasses originate from the ABL 50% of the time (Collaud Coen et al., 2011). I~~Moreover, it has been established that vertical export of airmasses above mountainous terrain is presently poorly represented in global CTMs (Henne et al., 2004). ~~In addition,~~ M~~m~~ean annual changes of GEOS-Chem methane agree with the observations in~~for~~ summer, during the influence of the ABL, with 0.33 ± 0.04 and 0.27 ± 0.08 % year^{-1} for Jungfraujoch and Zugspitze respectively. ~~and winter measurements show that with respectively 0.25 ± 0.06 and 0.33 ± 0.04 % year^{-1}, FTIR measurements and GEOS-Chem agree in summer, during the influence of the ABL, while they do not agree in winter. Indeed, FTIR winter measurements show a non-significant mean annual winter change of 0.10 ± 0.13 % year^{-1} while~~ In contrast, GEOS-Chem shows a mean annual winter change of respectively 0.23 ± 0.11 and 0.19 ± 0.09 % year^{-1} which agrees with Zugspitze change observations but not with Jungfraujoch changes.~~.~~ Since FTIR measurements and GEOS-Chem methane changes comparisons show a disagreement ~~agree~~ on the methane changes during winter~~in summer~~ at Jungfraujoch, ~~when under the influence of the ABL,~~ this seasonal analysis of changes of methane at mountaineous observations sites~~Jungfraujoch~~ emphasizes the current poor representation of summer versus winter thermal convection of air masses from the boundary layer to the free troposphere by the model.

This question has been addressed as well as the re-writing of this paragraph with the help of Dr. M. Collaud-Coen. Therefore, we would like to add Dr. Collaud-Coen to the list of co-authors.

In Page 10 line 13. This is not quite clear why "small annual changes of methane and smaller uncertainty ... complicates the agreement between the FTIR and GEOS-Chem...".

As the changes of methane remain quite small with respect to other atmospheric species (as an example, atmospheric ethane has increased of 4.9 ± 0.91 % year^{-1}; Franco et al., 2015), a slight discrepancy between two datasets and associated small uncertainty may easily lead to the conclusion of a disagreement.

In Page30 Table 3. Methane trends derived from FTIR measurements over 2005-2012 are higher for the stations that are located in the Northern Hemisphere than for sites in the Southern Hemisphere. In comparison to FTIR trends, GEOS-Chem simulations give us an opposite tendency: CH4 trends have lower values for the Northern Hemisphere. Could authors suggest any reasons of such inconsistency between observational and modeling estimations of CH4 trend?

From Figure 4 of the paper, there is no clear hemispheric bias in methane changes within the 2-σ uncertainty.

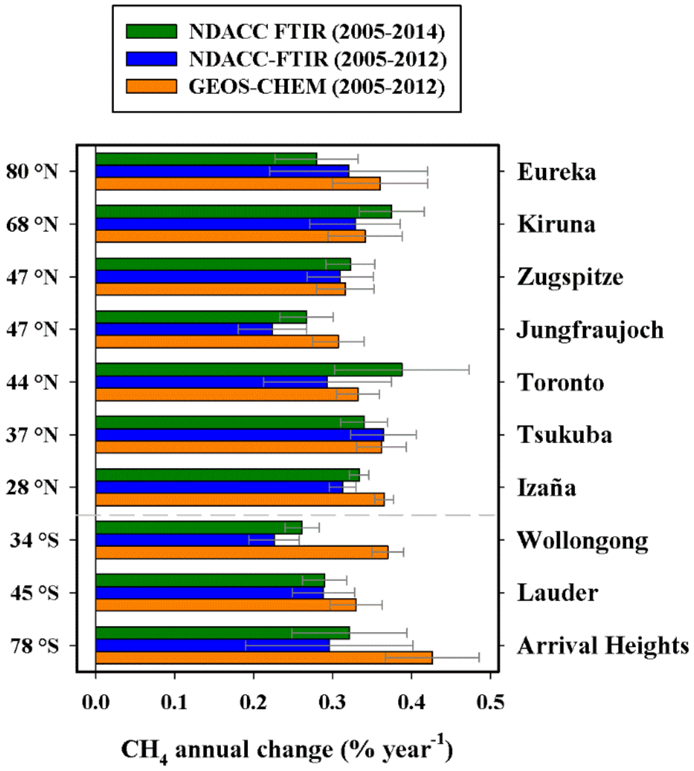

Figure 4: Methane total column mean annual change in % year^{-1} with respect to 2005.0 (2006.0 for Eureka), for the FTIR time series between 2005 and 2014 (in blue), the NDACC FTIR time series between 2005 and 2012 (in dark blue), and the GEOS-Chem simulation between 2005 and 2012 (in orange). Grey error bars represent 2-sigma uncertainty.

Technical corrections: Table 3. Column "GEOS-Chem trend [2005-2012]", row "Unit": please, check units.

The table has been edited accordingly.

Referee #3

General remarks:

1. Title: It might be nice to mention the used years "2005-2014" maybe something like:

"Ten years of atmospheric methane from ground-based NDACC FTIR observations between 2005-2014"

We agree that the title can be improved. Following Referee #1's comment and Referee #3's suggestions, the title of this paper will be edited to "The recent increase of atmospheric methane from ten years of ground-based NDACC FTIR observations since 2005."

2. Abstract: Some parts in the abstract could be written more concise and it might be important to mention that the work is based on total vertical column measurements.

The abstract will be edited accordingly :

" Changes of atmospheric methane total columns (CH_4) since 2005 have been evaluated using Fourier Transform Infrared (FTIR) solar observations performed at ten ground-based sites, affiliated to~~, all members of~~ the Network for Detection of Atmospheric Composition Change (NDACC). From this, we find an increase of atmospheric methane total columns of ~~that amounts to~~ 0.31 ± 0.03 % year^{-1}

(2-sigma level of uncertainty) for the 2005-2014 period. Comparisons with in situ methane measurements at both local and global scales show good agreement. We used the GEOS-Chem Chemical Transport Model tagged simulation that accounts for the contribution of each emission source and one sink in the total methane, simulated over ~~the~~ 2005-2012.~~ time period and based on emissions inventories and transport.~~ After regridding according to NDACC vertical layering using a conservative regridding scheme and smoothing by convolving with respective FTIR seasonal averaging kernels, the GEOS-Chem simulation shows an increase of atmospheric methane total columns of 0.35 ± 0.03 % year^{-1} between 2005 and 2012, which is in agreement with NDACC measurements over the same time period (0.30 ± 0.04 % year^{-1}, averaged over ten stations). Analysis of the GEOS-Chem tagged simulation allows us to quantify the contribution of each tracer to the global methane change since 2005. We find that natural sources such as wetlands and biomass burning contribute to the inter-annual variability of methane. However, anthropogenic emissions such as coal mining, and gas and oil transport and exploration, which are mainly emitted in the Northern Hemisphere and act as secondary contributors to the global budget of methane, have played a major role in the increase of atmospheric methane observed since 2005. Based on the GEOS-Chem tagged simulation, we discuss possible cause(s) for the increase of methane since 2005, which is still unexplained."

3. Retrieval: Some parts of the retrieval description might be done more easier and in a more common way: 1.For most reader a matrix is multiplied from the left side Please write the equation instead of the form, of maybe Rodgers 1990.
I admit that is the same, just the AVK matrix is defined in the transposed way A=AT.

The equation has been modified accordingly.

4. I do not understand the section 2.2.2 information content and as far as I know is the word INFORMATION CONTENT used for the Shannon information measure describing the increase of the information Rodgers 2000, which is here slightly different used and maybe not really useful but misleading as a title, maybe "Information analysis" might be better.
The title has been changed to "Degrees of freedom and vertical sensitivity range."

5. The eigenvector analysis might be an useful mathematical tool for many applications in OET, like transformation Sa-matrix to the identity…, but it might be difficult for the reader and not so easy to be understand in the more general constraint least square fitting approach which includes "Tihkonov"-regularisation. If you want to keep the eigenvectors figure, first of all you have to specify from which matrix you calculate eigenvectors and in which units you plot it: fraction or VMR. I assume you are doing it from VMR-Averaging kernels and uses VMR. As you work with ten sites I would like to see all of them, to know if this is a more or less harmonic set of retrievals or if you have to be more careful, if altitude dependent CH4 anomalies due to dynamics, stratospheric intrusions .. or other effects will be seen differently, by different sites. As the ten stations are not harmonized, I would like to see a simple averaging kernel for total column (AVKtot) of all ten station, either a typical or an average AVKtot. If you will emphasis on the altitude resolved information of the retrieval are important for this study, I would include the mean DOF in one of the tables maybe (Tab. 2), as this gives in addition information on the strength of the constraint at each site and retrieval strategy.
"established within the NDACC Infrared Working Group that the regularization strength of the methane retrieval strategy should be optimized so that the Degrees of Freedom For Signal (DOFS) is limited to a value of approximately 2 (Sussmann et al., 2011). As a consequence, the typical

information content of NDACC methane retrievals will allow us to retrieve tropospheric and stratospheric columns, as displayed in Fig. 3.", a more common way to look at two partial columns would be to plot the two partial column averaging kernels and the total column averaging kernel.

As requested, an averaged value of the DOFS along with its associated 1-σ uncertainty has been added to Table A1. The merged-layer kernels, while not included in the new figure as the 10 vectors prevents us to analyze the figure clearly, show for all sites a very similar pattern, with values close to one from the ground/surface up to 20 km. Figure 3 has been edited as follows :

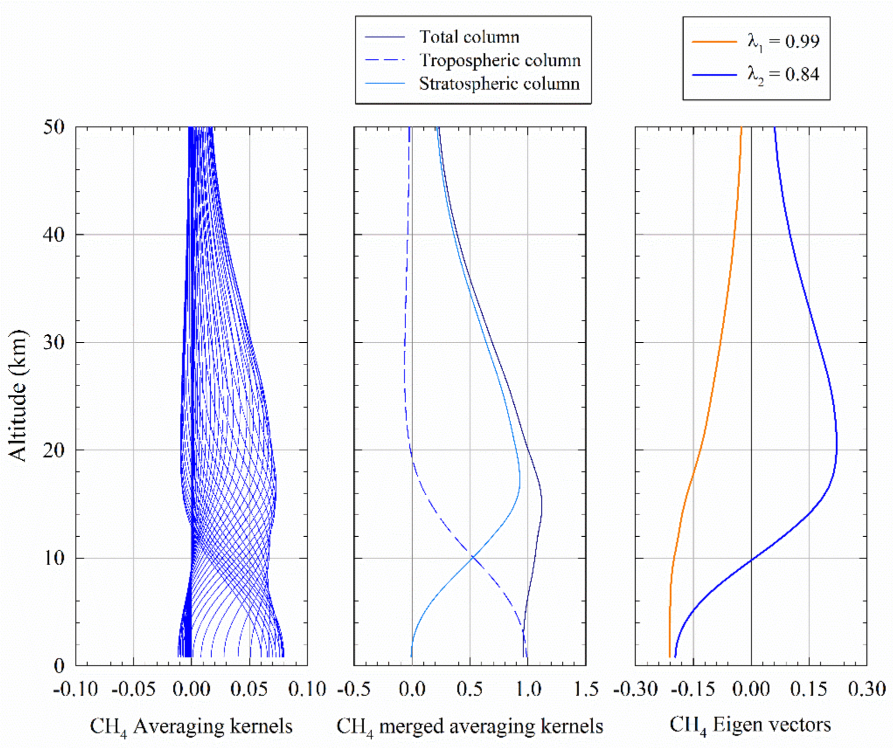

Figure 3: Typical NDACC methane retrieval. From left to right. First panel : typical individual (blue curves) CH_4 mixing ratio averaging kernels. Second panel : Merged (shades of blue curves) CH_4 mixing ratio averaging kernels. For merged-layer kernels, corresponding atmospheric column are specified in the legend box. Third panel : corresponding two first eigenvectors. Associated eigenvalues are given in the legend.

6. optional: Jungfraujoch and Zugspitze, see the same pattern of annual resolved changes: Especially prominent is the huge difference between 2010 and 2011: That is really interesting and seems consistent for both the MODEL and hopefully also with the FTIR time series. Could you proof this with the FTIR-Model difference? Maybe with a model-control run using an average change, which would result in a MODEL-FTIR residual with a similar structure than the red line in figure 6.

The proximity of both Jungfraujoch and Zugspitze stations (~250 km away and 600m altitude difference) explains how GEOS-Chem simulates similar yearly changes. However, as stated above, CTMs poorly represent processes occurring at a local scale such as thermally driven transport (Forrer et al., 2000; Okamoto and Tanimoto, 2016), the cause of the differences between observed changes at both stations.

7. Fig 2 is already included in Fig. 5 therefore I would suggest show in Fig 2 the absolute columns not anomalies, either the daily means or even the individual measurements.

As methane total columns cover different range of values from one station to another (mostly depending on the altitude of the station), we would like to keep the current version of the figure in order to keep homogeneous axes from one panel to another.

8. Table 2: interference species: please defined if the gases in your list are the simultaneously fitted gases or all in addition simulated interference gases, you could replace the column with the interference gases in the main article by DOF of each site retrieval strategy. Maybe provide a supplement, where you add more about the 10 retrieval strategies with exact micro windows fitted, prefitted and simulated interference gases.

Following the reviewer suggestion, Table 2 will be moved to an appendix (now Appendix A) where the limits of the windows and their corresponding interfering species will be mentioned. The averaged DOFS and their associated 2σ-uncertainties for each dataset have been added.

9. QA/QC: Looking on the time series and the different results of the model, which explain some sites quite well and other less, I wonder if the operators might use different quality selection of spectra and retrieval results and therefore some time series show a higher scatter, as harmonisation of quality control (QC) might be too much effort at this stage, but it may be possible to include just a table which sumarise, the different QC criteria and help the reader to evaluate if only local effects will produce the heterogen image Fig. 5, or maybe also individual quality filters.

That is correct, QC is not yet harmonized in NDACC. However, due to different latitude, altitude, humidity and instrumental performances, signal to noise of the data will still be different, differences that are captured by the error estimates.

From the ten time series illustrated on Figure 5, higher scattered data is more pronounced for urban sites such as Toronto and Wollongong. The scatter is mainly due to local pollutions and different wind direction rather than due to quality check of the spectra. For instance, the anomaly for Toronto is up to 15 % which is beyond the error estimate.

However, it is important here to emphasize on the fact that the bootstrap resampling method minimizes the impact of the scattered data on the computed methane changes between 2005 and 2014.

10. Table 3: Units column 7 and 8 have to be exchanged: "molec. cm- Yr-1”<->” The molec.cm
−2yr {−1 the 2 is missing.
The manuscript will be modified accordingly.

References

Collaud Coen, M., Weingartner, E., Furger, M., Nyeki, S., Prévôt, A. S. H., Steinbacher, M. and Baltensperger, U.: Aerosol climatology and planetary boundary influence at the Jungfraujoch analyzed by synoptic weather types, Atmos. Chem. Phys., 11(12), 5931–5944, doi:10.5194/acp-11-5931-2011, 2011.
Forrer, J., Rüttimann, R., Schneiter, D., Fischer, A., Buchmann, B. and Hofer, P.: Variability of trace gases at the high-Alpine site Jungfraujoch caused by meteorological transport processes, J. Geophys. Res. Atmos., 105(D10), 12241–12251, doi:10.1029/1999JD901178, 2000.
Franco, B., Bader, W., Toon, G. C., Bray, C., Perrin, A., Fischer, E. V., Sudo, K., Boone, C. D., Bovy, B., Lejeune, B., Servais, C. and Mahieu, E.: Retrieval of ethane from ground-based FTIR solar spectra using improved spectroscopy: Recent burden increase above Jungfraujoch, J. Quant. Spectrosc.

Radiat. Transf., 160, 36–49, doi:10.1016/j.jqsrt.2015.03.017, 2015.

Gardiner, T., Forbes, A., de Mazière, M., Vigouroux, C., Mahieu, E., Demoulin, P., Velazco, V., Notholt, J., Blumenstock, T., Hase, F., Kramer, I., Sussmann, R., Stremme, W., Mellqvist, J., Strandberg, A., Ellingsen, K. and Gauss, M.: Trend analysis of greenhouse gases over Europe measured by a network of ground-based remote FTIR instruments, Atmos. Chem. Phys., 8(22), 6719–6727, doi:10.5194/acp-8-6719-2008, 2008.

Henne, S., Furger, M. and Prévôt, A. H.: Climatology of Mountain Venting–Induced Elevated Moisture Layers in the Lee of the Alps, J. Appl. Meteorol., 44(5), 620–633, doi:10.1175/JAM2217.1, 2005.

Henne, S., Brunner, D., Folini, D., Solberg, S., Klausen, J. and Buchmann, B.: Assessment of parameters describing representativeness of air quality in-situ measurement sites, Atmos. Chem. Phys., 10(8), 3561–3581, doi:10.5194/acp-10-3561-2010, 2010.

Ketterer, C., Zieger, P., Bukowiecki, N., Collaud Coen, M., Maier, O., Ruffieux, D. and Weingartner, E.: Investigation of the Planetary Boundary Layer in the Swiss Alps Using Remote Sensing and In Situ Measurements, Boundary-Layer Meteorol., 151(2), 317–334, doi:10.1007/s10546-013-9897-8, 2014.

Kulawik, S. S., Wunch, D., O’Dell, C., Frankenberg, C., Reuter, M., Oda, T., Chevallier, F., Sherlock, V., Buchwitz, M., Osterman, G., Miller, C., Wennberg, P., Griffith, D. W. T., Morino, I., Dubey, M., Deutscher, N. M., Notholt, J., Hase, F., Warneke, T., Sussmann, R., Robinson, J., Strong, K., Schneider, M. and Wolf, J.: Consistent evaluation of GOSAT, SCIAMACHY, CarbonTracker, and MACC through comparisons to TCCON, Atmos. Meas. Tech. Discuss., 8(6), 6217–6277, doi:10.5194/amtd-8-6217-2015, 2015.

Okamoto, S. and Tanimoto, H.: A review of atmospheric chemistry observations at mountain sites, Prog. Earth Planet. Sci., 3(1), 34, doi:10.1186/s40645-016-0109-2, 2016.

Rinsland, C. P., Goldman, A., Elkins, J. W., Chiou, L. S., Hannigan, J. W., Wood, S. W., Mahieu, E. and Zander, R.: Long-term trend of CH4 at northern mid-latitudes: Comparison between ground-based infrared solar and surface sampling measurements, J. Quant. Spectrosc. Radiat. Transf., 97(3), 457–466, doi:10.1016/j.jqsrt.2005.07.002, 2006.

Sepúlveda, E., Schneider, M., Hase, F., García, O. E., Gomez-Pelaez, a., Dohe, S., Blumenstock, T. and Guerra, J. C.: Long-term validation of tropospheric column-averaged CH_4 mole fractions obtained by mid-infrared ground-based FTIR spectrometry, Atmos. Meas. Tech., 5(6), 1425–1441, doi:10.5194/amt-5-1425-2012, 2012.

Solomon, S., Rosenlof, K. H., Portmann, R. W., Daniel, J. S., Davis, S. M., Sanford, T. J. and Plattner, G.-K.: Contributions of Stratospheric Water Vapor to Decadal Changes in the Rate of Global Warming, Science (80-.)., 327(5970), 1219–1223, doi:10.1126/science.1182488, 2010.

Stocker, T. F., Qin, D., Plattner, G.-K., Tignor, M., Allen, S. K., Boschung, J., Nauels, A., Xia, Y., Bex, V. and Midgley, P. M.: The Physical Science Basis. Contribution of Working Group I to the Fifth Assessment Report of the Intergovernmental Panel on Climate Change, Cambridge., Cambridge, United Kingdom and New York, NY, USA., 2013.

Sussmann, R., Forster, F., Rettinger, M. and Jones, N.: Strategy for high-accuracy-and-precision retrieval of atmospheric methane from the mid-infrared FTIR network, Atmos. Meas. Tech., 4(9), 1943–1964, doi:10.5194/amt-4-1943-2011, 2011.

Zellweger, C., Ammann, M., Buchmann, B., Hofer, P., Lugauer, M., Rüttimann, R., Streit, N., Weingartner, E. and Baltensperger, U.: Summertime NO y speciation at the Jungfraujoch, 3580 m above sea level, Switzerland, J. Geophys. Res. Atmos., 105(D5), 6655–6667, doi:10.1029/1999JD901126, 2000.

Zellweger, C., Forrer, J., Hofer, P., Nyeki, S., Schwarzenbach, B., Weingartner, E., Ammann, M. and Baltensperger, U.: Partitioning of reactive nitrogen (NOy) and dependence on meteorological conditions in the lower free troposphere, Atmos. Chem. Phys., 3(3), 779–796, doi:10.5194/acp-3-779-2003, 2003.

Relevant changes

1- From the reviewer’s comments and suggestions, we would like to edit the title to : "The recent increase of atmospheric methane from Ten years of atmospheric methane from ground-based NDACC FTIR observations since 2005."

2- In addition, in order to address one of the reviewer’s question, we contacted Dr. M. Collaud-Coen who provided substantial information. Therefore, in agreement with Editor Hal Maring, we would like to include her as one of the co-author (affiliation Federal Office of Meteorology and Climatology, MeteoSwiss, 1530 Payerne, Switzerland).

The new list of co-author and affiliations goes as follows :

Whitney Bader[1,2], Benoît Bovy[1], Stephanie Conway[2], Kimberly Strong[2], Dan Smale[3], Alexander J. Turner[4], Thomas Blumenstock[5], Chris Boone[6], Martine Collaud-Coen[7], Ancelin Coulon[8], Omaira Garcia[9], David W. T. Griffith[10], Frank Hase[5], Petra Hausmann[11], Nicholas Jones[10], Paul Krummel[12], Isao Murata[13], Isamu Morino[14], Hideaki Nakajima[14], Simon O’Doherty[15], Clare Paton-Walsh[10], John Robinson[3], Rodrigue Sandrin[2], Matthias Schneider[5], Christian Servais[1], Ralf Sussmann[11] and Emmanuel Mahieu[1].

1 Institute of Astrophysics and Geophysics, University of Liège, Liège, Belgium
2 Department of Physics, University of Toronto, Toronto, ON, M5S 1A7, Canada
3 National Institute of Water and Atmospheric Research, NIWA, Lauder, New Zealand
4 School of Engineering and Applied Sciences, Harvard University, Cambridge, MA, USA
5 Karlsruhe Institute of Technology (KIT), Institute of Meteorology and Climate Research (IMK-ASF), Karlsruhe, Germany
6 Department of Chemistry, University of Waterloo, Waterloo, ON, N2L 3G1, Canada
7 Federal Office of Meteorology and Climatology, MeteoSwiss, 1530 Payerne, Switzerland
8 Institute for Atmospheric and Climate Science, ETH Zurich, Zurich, Switzerland
9 Izana Atmospheric Research Centre (IARC), Agencia Estatal de Meteorologia (AEMET), Spain
10 School of Chemistry, University of Wollongong, Australia
11 Karlsruhe Institute of Technology, IMK-IFU, Garmisch-Partenkirchen, Germany
12 CSIRO Oceans & Atmosphere, Aspendale, Victoria, Australia
13 Graduate School of Environment Studies, Tohoku University, Sendai 980-8578, Japan
14 National Institute for Environmental Studies (NIES), Tsukuba, Ibaraki 305-8506, Japan
15 Atmospheric Chemistry Research Group (ACRG), School of Chemistry, University of Bristol, UK

3- Following the reviewer's comments and suggestions and in order to be more comprehensive about the retrieval strategies of each station, Table 2 will be moved to an appendix (now Appendix A).

Appendix A - NDACC FTIR retrieval strategies

Table A1 summarizes the retrieval parameters for methane for each station. FTIR measurements are analyzed as recommended either by Rinsland et al. (2006), Sussmann et al. (2011), or Sepúlveda et al. (2012). The spectral microwindows limits for the Eureka, Zugspitze, Toronto and Wollongong stations are based on Sussmann et al., (2011) and use the Hitran-2000 spectroscopic database including 2001 update release (Rothman et al., 2003) except for Toronto where Hitran 2008 was employed (Rothman et al., 2009). The microwindows used for the Kiruna, Jungfraujoch, Izaña observations are based on Sepulveda et al. (2012). For all interfering species, Hitran 2008 parameters are used. For methane, ad hoc adjustments performed by KIT, IMK-ASF are used (D. Dubravica, priv. comm., Dec 2012; see also Dubravica et al., 2013). Finally, the microwindows used for the Lauder and Arrival Heights observations are based on Rinsland et al. (2006). In order to better appraise the relatively low humidity rates at Jungfraujoch, a pre-fitting of the two microwindows (2611.60 - 2613.35 and 2941.65 - 2941.89) dedicated to water vapour and its isotopologue HDO is performed and used as a priori for the actual retrieval.

A priori profiles for target and interfering molecules are based on the Whole Atmosphere Community Climate Model (version 5 or 6, WACCM, e.g. Chang et al., 2008) climatology, except for Tsukuba, Lauder and Arrival Heights. A priori profile for Tsukuba retrievals include monthly averaged profiles made from airplane measurements over Japan by the National Institute of Environmental Studies, Japan (NIES, http://www.nies.go.jp/index-e.html). A priori profile for Lauder retrieval include annual mean of measurements from the Microwave Limb Sounder (MLS, https://mls.jpl.nasa.gov/) and the Halogen Occultation Experiment (HALOE, http://haloe.gats-inc.com/home/index.php) onboard the Upper Atmosphere Research Satellite (UARS, http://uars.gsfc.nasa.gov/) at 44°S in the framework of the UARS Reference Atmosphere Project (URAP, Grooß and Russell, 2005). A priori for Arrival Heights retrievals include zonal mean of measurements from the Atmospheric Trace Molecule Spectroscopy Experiment (ATMOS) Spacelab 3 over the 14-65 km altitude range (Gunson et al., 1996). As mentioned in the Sect. 2.2.2. of this paper, a Tikhonov regularization (Tikhonov, 1963) is used and optimized in order to limit the value of the Degrees of Freedom For Signal (DOFS) to a value of approximately 2 (Sussmann et al., 2011) except for Lauder and Arrival Heights that uses an Optimal Estimation Method (OEM) based on the formalism of Rodgers (1990). Averaged DOFS value and associated 1-σ uncertainty are given in the last column of Table A1.

Station	**Retrieval code**	**Retrieval windows (cm^{-1})**	**Interfering gases**	**A priori & regularization**	**Linelist**	**Averaged DOFS**
EUR	SFIT-4	2613.7 – 2615.4	HDO CO_2	WACCM v6	HIT-08	2.31 ± 0.66
		2835.5 – 2835.8	HDO	Tikhonov L_1		
		2921.0 – 2921.6	HDO H_2O NO_2			
KIR	PROFFIT	2611.6 - 2613.35	HDO CO_2 N_2O (no CH_4)	WACCM v6	[f] ad hoc CH_4	2.35 ± 0.29
		2613.7 - 2615.4	HDO CO_2 O_3 N_2O	Tikhonov L_1	HIT-08	
		2835.55 - 2835.8	HDO O_3 N_2O			
		2903.82 - 2903.925	H_2O HDO O_3 NO_2 N_2O OCS HCl			
		2914.7 - 2915.15	H_2O HDO O_3 NO_2 OCS HCl			
		2941.51 - 2942.22	H_2O O_3 OCS (no CH_4)			
ZUG	PROFFIT	2613.7 - 2615.4	HDO CO_2	WACCM v6	[g] HIT-00	1.93 ± 0.32
		2835.5 - 2835.8	HDO	Tikhonov L_1		
		2921.0 - 2921.6	HDO H_2O NO_2			
JFJ	SFIT-2 v3.94	2611.60 - 2613.35	HDO CO_2 (no CH_4)	WACCM v6	[f] ad hoc CH_4	2.37 ± 0.46
		2613.7 - 2615.4	HDO CO_2 O_3	Tikhonov L_1	HIT-08	
		2835.55 - 2835.80	HDO O_3			
		2903.82 - 2903.925	H_2O HDO O_3 NO_2			
		2914.70 - 2915.15	H_2O HDO O_3 NO_2 HCl			
		2941.65 - 2941.89	H_2O O_3 (no CH_4)			
TOR	SFIT-4	2613.7 - 2615.4	HDO CO_2	WACCM v6	HIT-08	2.05 ± 0.69
		2835.5 - 2835.8	HDO	Tikhonov L_1		
		2921.0 - 2921.6	HDO H_2O NO_2			
TSU	SFIT-2 v3.94	2613.7 - 2615.4	HDO CO_2	[h]NIES Airplane	HIT-00	2.73 ± 0.18
		2835.5 - 2835.8	HDO	Tikhonov L_1		
		2921.0 - 2921.6	HDO H_2O NO_2			
IZA	PROFFIT	2611.6 - 2613.35	HDO CO_2 N_2O (no CH_4)	WACCM v6	[f] ad hoc CH_4	2.42 ± 0.28
		2613.7 - 2615.4	HDO CO_2 O_3 N_2O	Tikhonov L_1	HIT-08	
		2835.55 - 2835.8	HDO O_3 N_2O			
		2903.82 - 2903.925	H_2O HDO O_3 NO_2 N_2O OCS HCl			
		2914.7 - 2915.15	H_2O HDO O_3 NO_2 OCS HCl			
		2941.51 - 2942.22	H_2O O_3 OCS (no CH_4)			
WOL	SFIT-2 v3.94	2613.7 - 2615.4	HDO CO_2	WACCM v5	HIT-00	1.81 ± 0.28
		2835.5 - 2835.8	HDO	Tikhonov L_1		
		2921.0 - 2921.6	HDO H_2O NO_2			
LAU	SFIT-2 v3.82	2650.85 - 2651.25	HDO	[j] URAP at 44°S	HIT-00	2.96 ± 0.73
		2666.95 - 2667.35	HDO	[k] OEM		
		2673.90 - 2674.41	HDO			

AHT	SFIT-2 v3.82	2650.85 - 2651.25	HDO		[1]ATMOS zonal mean OEM	HIT-00	3.54 ± 0.76
		2666.95 - 2667.35	HDO				
		2673.90 - 2674.41	HDO				

Table A1: Retrieval parameters for each station.

The recent increase of atmospheric methane from ~~T~~ten years of~~of~~ ~~atmospheric methane from~~ ground-based NDACC FTIR observations since 2005

Whitney Bader[1,2], Benoît Bovy[1], Stephanie Conway[2], Kimberly Strong[2], Dan Smale[3], Alexander J. Turner[4], Thomas Blumenstock[5], Chris Boone[6], Martine Collaud Coen[7], Ancelin Coulon[8~~7~~], Omaira Garcia[9~~8~~], David W. T. Griffith[10~~9~~], Frank Hase[5], Petra Hausmann[11~~0~~], Nicholas Jones[10~~9~~], Paul Krummel[12~~11~~], Isao Murata[13~~12~~], I. Morino[14~~13~~], Hideaki Nakajima[14~~13~~], Simon O'Doherty[15~~4~~], Clare Paton-Walsh[10~~9~~], John Robinson[3], Rodrigue Sandrin[2], Matthias Schneider[5], Christian Servais[1], Ralf Sussmann[11~~0~~] and Emmanuel Mahieu[1]

Mis en forme : Exposant

[1]Institute of Astrophysics and Geophysics, University of Liège, Liège, Belgium
[2]Department of Physics, University of Toronto, Toronto, ON, M5S 1A7, Canada
[3]National Institute of Water and Atmospheric Research, NIWA, Lauder, New Zealand
[4]School of Engineering and Applied Sciences, Harvard University, Cambridge, MA, USA
[5]Karlsruhe Institute of Technology (KIT), Institute of Meteorology and Climate Research (IMK-ASF), Karlsruhe, Germany
[6]Department of Chemistry, University of Waterloo, Waterloo, ON, N2L 3G1, Canada
[7]Federal Office of Meteorology and Climatology, MeteoSwiss, 1530 Payerne, Switzerland
[8~~7~~]Institute for Atmospheric and Climate Science, ETH Zurich, Zurich, Switzerland
[9~~8~~]Izana Atmospheric Research Centre (IARC), Agencia Estatal de Meteorologia (AEMET), Spain
[10~~9~~]School of Chemistry, University of Wollongong, Australia
[11~~0~~]Karlsruhe Institute of Technology, IMK-IFU, Garmisch-Partenkirchen, Germany
[12~~1~~]CSIRO Oceans & Atmosphere, Aspendale, Victoria, Australia
[13~~2~~]Graduate School of Environment Studies, Tohoku University, Sendai 980-8578, Japan
[14~~3~~]National Institute for Environmental Studies (NIES), Tsukuba, Ibaraki 305-8506, Japan
[15~~4~~]Atmospheric Chemistry Research Group (ACRG), School of Chemistry, University of Bristol, UK

Mis en forme : Exposant

Correspondence to: Whitney Bader (wbader@atmosp.physics.utoronto.ca)

Abstract

Changes of atmospheric methane total columns (CH_4) since 2005 have been evaluated using Fourier Transform Infrared (FTIR) solar observations performed at ten ground-based sites, affiliated to~~, all members of~~ the Network for Detection of Atmospheric Composition Change (NDACC). From this, we find an increase of atmospheric methane total columns of ~~that amounts to~~ 0.31 ± 0.03 % year^{-1} (2-sigma level of uncertainty) for the 2005-2014 period. Comparisons with in situ methane measurements at both local and global scales show good agreement. We used the GEOS-Chem Chemical Transport Model tagged simulation that accounts for the contribution of each emission source and one sink in the total methane, simulated over ~~the~~ 2005-2012, ~~time period and based on emissions inventories and transport.~~ After regridding according to NDACC vertical layering using a conservative regridding scheme and smoothing by convolving with respective FTIR seasonal averaging kernels, the GEOS-Chem simulation shows an increase of atmospheric methane total columns of 0.35 ± 0.03 % year^{-1} between 2005 and 2012, which is in agreement with NDACC measurements over the same time period (0.30 ± 0.04 % year^{-1}, averaged over ten stations). Analysis of the GEOS-Chem tagged simulation allows us to quantify the contribution of each tracer to the global methane change since 2005. We find that natural sources such as wetlands and biomass burning contribute to the inter-annual variability of methane. However, anthropogenic emissions such as coal mining, and gas and oil transport and exploration, which are mainly emitted in the Northern Hemisphere and act as secondary contributors to the global budget of methane, have played a major role in the increase of atmospheric methane observed since 2005. Based on the GEOS-Chem tagged simulation, we discuss possible cause(s) for the increase of methane since 2005, which is still unexplained.

1 Introduction

Atmospheric methane (CH_4), a relatively long-lived atmospheric species with a lifetime of 8-10 years (Kirschke et al., 2013), is the second most abundant anthropogenic greenhouse gas, with a radiative forcing (RF) of 0.97 ± 0.23 W m^{-2} (including indirect radiative forcing associated with the production of tropospheric ozone and stratospheric water vapor; Stocker et al., 2013)~~),~~ after CO_2 (RF in 2011: 1.68 ± 0.35 W m^{-2}, Stocker et al., 2013). Approximately one-fifth of the increase in radiative forcing by human-linked greenhouse gases since 1750 is due to methane (Nisbet et al., 2014). Identified emission sources include anthropogenic and natural contributions. Human activities associated with the agricultural and the energy sectors are the main sources of anthropogenic methane through enteric fermentation of livestock (17 %), rice cultivation (7 %), for the former, and coal mining (7 %), oil and gas exploitation (12 %), and waste management (11 %), for the latter. On the other hand, natural sources of methane include wetlands (34 %), termites (4 %), methane hydrates and ocean (3 %) along with biomass burning (4 %), a source of atmospheric methane that is both natural and anthropogenic. The above-mentioned estimated contributions to the atmospheric content of methane are based on Chen and Prinn (2006), Fung et al. (1991), Kirschke et al. (2013) and on emission inventories used for the GEOS-Chem v9-02 methane simulation (Turner et al., 2015), although it is worth noting that the global budget of methane remain insufficiently understood ~~and it is worth noting that these figures are still affected by significant uncertainties~~.

Methane is depleted at the surface by consumption by soil bacteria, in the marine boundary layer by reaction with chlorine atoms, in the troposphere by oxidation with the hydroxyl radical (OH), and in the stratosphere by reaction with chlorine atoms, $O(^1D)$, OH, and by photodissociation (Kirschke et al., 2013). Due to its sinks, methane has important chemical impacts on the atmospheric composition. In the troposphere, oxidation of methane is a major regulator of OH (Lelieveld, 2002) and is a source of hydrogen and of tropospheric ozone precursors such as formaldehyde and carbon monoxide (Montzka et al., 2011). In the stratosphere, methane plays a central role as a sink for chlorine atoms and as a source of stratospheric water vapor, an important driver of decadal global surface climate change (Solomon et al., 2010). Given its atmospheric lifetime, its impact on radiative forcing and on atmospheric chemistry, methane is one of the primary targets for regulation of greenhouse gas emissions and climate change mitigation.

As a result of growing anthropogenic emissions, atmospheric methane showed prolonged periods of increase over the past three decades (World Meteorological Organization, 2014). From the 1980s until the beginning of the 1990s, atmospheric methane was rising sharply by about ~ 0.7 % $year^{-1}$ (Nisbet et al., 2014) but stabilized during the 1999-2006 time period (Dlugokencky, 2003). Many studies were dedicated to the analysis of methane trends, in particular the stabilization of methane concentrations between 1999 and 2006, and various scenarios have been suggested. They include reduced global fossil-fuel-related emissions (Aydin et al., 2011; Chen and Prinn, 2006; Simpson et al., 2012; Wang et al., 2004), a compensation between increasing anthropogenic emissions and decreasing wetland emissions (Bousquet et al., 2006), and/or significant (Rigby et al., 2008) to small (Montzka et al., 2011) changes in OH concentrations. However, Pison et al. (2013) emphasized the need for a comprehensive and precisely quantified methane budget for its proper closure and the development of realistic future climate scenarios.

Since 2005-2006, a renewed increase of atmospheric methane has been observed and widely discussed in many studies (Bloom et al., 2010; Dlugokencky et al., 2009; Frankenberg et al., 2011; Hausmann et al., 2016; Helmig et al., 2016; Montzka et al., 2011; Rigby et al., 2008; Schaefer et al., 2016; Spahni et al., 2011; Sussmann et al., 2012; van der Werf et al., 2010), leading to various hypotheses. In this work, for the first time, we report of an increase of methane as observed since 2005 at a suite of NDACC sites distributed worldwide and operating Fourier Transform InfraRed (FTIR) Spectrometers. The paper is organized as follows: Sect. 2 includes a brief description of the ten participating sites, and the retrieval strategy and information content of the FTIR measurements. Sect. 3 focuses on the methane changes since 2005 as derived from the NDACC FTIR measurements, and the GEOS-Chem model, along with comparisons between both model and observations. This section also provides a source-oriented analysis of the recent increase of methane using the GEOS-Chem tagged simulation. Finally, Sect. 4 discusses the potential source(s) responsible for the observed increase of methane since the mid-2000s.

2 NDACC FTIR observations

The international Network for the Detection of Atmospheric Composition Change (NDACC) is dedicated to observing and understanding of the physical and chemical state of the stratosphere and troposphere. Its priorities include the detection of trends in atmospheric composition, understanding their impacts on the stratosphere and troposphere, and establishing links between climate change and atmospheric composition.

2.1 Observation sites

Ground-based NDACC FTIR measurements of methane obtained at ten globally distributed observation sites are presented in this study. These sites, displayed on Fig. 1 and whose location is detailed in Table 1 are located from North to South in Eureka (Arctic, Canada), Kiruna (Sweden), Zugspitze (Germany), Jungfraujoch (Switzerland), Toronto (Canada), Tsukuba (Japan), Izaña (Canary Island, Spain), Wollongong (Australia), Lauder (New Zealand), Arrival Heights (Antarctica). Most of the FTIR data is available on the NDACC database (http://www.ndsc.ncep.noaa.gov/data/).

The Eureka (EUR, Fogal et al., 2013) station is located in the Canadian high Arctic, at 610 m a.s.l. on Ellesmere Island in the northern Canadian Archipelago. The station is located along the Slidre Fjord and is surrounded by complex topography (Cox et al., 2012). This topography, along with its proximity to the Greenland Ice Sheet and atmospheric conditions, make this station ideal for infrared solar measurements in the Arctic as it is frequently under the influence of cold and dry air from central Arctic and the Greenland Ice Sheet (Cox et al., 2012). Routine solar infrared measurements are performed from late February to late October), no lunar measurements are taken during polar night (Batchelor et al., 2009).

The Kiruna (KIR) site is located in the boreal forest region of Northern Sweden. The spectrometer is operated in the building of the IRF (Institute för Rymdfysik/Swedish Institute of Space Physics), at an altitude of 420 m, about 10 km away from the center of Kiruna~~, the northernmost town of Sweden~~. The local population and traffic density is low, so the FTIR site is not significantly affected by local anthropogenic emissions. The location just inside the polar circle is especially suited for the study of the Arctic polar stratosphere, because the break in solar absorption observations is still rather short, while the stratospheric polar vortex frequently covers Kiruna in early spring. The solar absorption spectra were obtained with a Bruker IFS-120HR since 1996. In 2007, an electronic upgrade to a Bruker IFS-125HR was implemented. Routine solar infrared measurements are performed between mid-January and mid-November, no lunar measurements are taken during polar night.

The Zugspitze site (ZUG, Sussmann and Schäfer, 1997) is located on the southern slope of the Zugspitze mountain, the highest mountain of the German Alps (2964 m a.s.l.), at the Austrian border near the town of Garmisch-Partenkirchen (720 m a.s.l.). Its high-altitude offers an excellent location for long-term trace gas measurements under unperturbed background atmospheric conditions and exhibits a very low level of integrated water vapor.

The Jungfraujoch (JFJ, Zander et al., 2008) station is located in the Swiss Alps at 3580 m altitude on the saddle between the Jungfrau (4158 m a.s.l.) and the Mönch (4107 m a.s.l.) summits. This station offers unique conditions for infrared solar observations because of weak local pollution (no major industries within 20 km) and very high dryness due to the high-altitude and the presence of the Aletsch Glacier in its immediate vicinity. The Jungfraujoch station allows the investigation of the atmospheric background conditions over central Europe and the mixing of air masses between the planetary boundary layer and the free troposphere (Reimann, 2004).

The Toronto (TOR) station is located in the core of the ~~mega~~city of Toronto, Ontario, Canada at 174 m a.s.l. where regular solar measurements began in 2002. In contrast to most NDACC stations, the Toronto station is highly affected by the densely populated areas of the city of Toronto itself (the center of Canada's largest population) and the cities and industrial centers of the North Eastern United States, enabling measurements of tropospheric pollutants (Whaley et al., 2015). In addition, the station's location makes it well suited for measurements of mid-latitude stratospheric ozone, related species, and greenhouse gases (Wiacek et al., 2007).

The Tsukuba (TSU) station is located in a suburban area (around 50 km from Tokyo) and in a large plain with many rice paddies at an altitude of 31 m. The station occasionally captures local pollution and is affected by high humidity during the summer season. The Tsukuba solar absorption spectra were obtained with a Bruker IFS-120HR from May 2001 to March 2010, and replaced by a Bruker IFS-125HR in April 2010.

The Izaña observatory (IZA, http://www.izana.org), is located on the top of a mountain plateau in the Teide National Park on the Island of Tenerife. It is usually located above a strong subtropical temperature inversion layer (generally well established between 500 and 1500 m a.s.l.) and clean-air and clear-sky conditions are prevailing year-round. Consequently it offers excellent conditions for the remote sensing of trace gases and aerosols under “free troposphere” conditions and for atmospheric observations. Due to its geographic location, it is particularly valuable for the investigation of dust transport from Africa to the North Atlantic, and large-scale transport from the tropics to higher latitudes. In addition, during daytime the strong insolation generates a slight upslope flow of air originating from below the inversion layer (from a woodland that surrounds the station at a lower altitude, Sepúlveda et al., 2012). The solar absorption spectra were obtained with a Bruker IFS 120M over 1999-2004, then with a Bruker IFS 125HR thereafter (Sepúlveda et al., 2012).

Wollongong (WOL, Griffith et al., 1998) is a coastal city about 80 km south of the metropolis of Sydney. Its urban location, in proximity to Sydney and local coal mining operations means that enhanced levels of CH_4 are measured from time to time. Climatologically the winds are weak (<4 m s-1); during the Southern Hemisphere winter the site largely samples continental airmasses from the west, with summer afternoon sea-breezes from the East-Northeast (Fraser et al., 2011). The solar absorption spectra were obtained with a Bomem DA8 from 1995 to 2007 (Griffith et al., 1998) and with a Bruker IFS 125/HR from 2007 onwards.

The Lauder (LAU) atmospheric research station is located in the Manuherikia valley, Central Otago, New Zealand. The site experiences a continental climate of hot dry summers and cool winters with a predominating westerly wind. The site is sparsely populated and remote from any major industries with non-intense agricultural and horticulture as the mainstay of economic activity.

The Arrival Heights (AHT) atmospheric laboratory is located 3 km north of McMurdo and Scott Base stations on Hut Point Peninsula, the southern volcanic peninsula of Ross Island. With minimal exposure to local anthropogenic pollution and sources, methane measurements conducted at Arrival Heights are representative of a well-mixed boundary layer and free troposphere. Located at 78°S, Arrival Heights is periodically underneath the polar vortex depending on the season, polar vortex shape and angular rotation velocity. Climatological surface meteorological conditions experienced at Arrival Heights are similar to that of Scott Base (Turner et al., 2004). Routine solar infrared measurements are performed during the austral spring and summer seasons (late August to mid-April) no measurements are taken during polar night.

2.2 FTIR Observations of methane

2.2.1 Retrieval strategies

A retrieval strategy for the inversion of atmospheric methane time series from ground-based FTIR observations has been carefully developed and optimized for each station. However, it is worth mentioning that given the remaining inconsistencies affecting the methane spectroscopic parameters, even in the latest editions of HITRAN (Rothman et al., 2013 and references therein), the harmonization of retrieval strategies for methane for the whole infrared working group of NDACC is still ongoing. To this day, FTIR measurements are analyzed as recommended either by Rinsland et al. (2006), Sussmann et al. (2011), or Sepúlveda et al. (2012). Table B1~~2~~ presents the retrieval parameters used for each station. The retrieval codes PROFFIT (Hase, 2000) and SFIT-2/SFIT-4 (Rinsland et al., 1998) have been shown to provide consistent results for tropospheric and stratospheric species (Duchatelet et al., 2010; Hase et al., 2004). The time series produced using the strategies described in Table 2 are illustrated in Fig. 2. In order to better illustrate the observed increase of methane total columns, ~~T~~the various panels show daily mean methane time series expressed as anomalies with respect to a reference column in 2005.0 (2006.0 for the Eureka station), according to the following equation :

$$Anomaly = \frac{C-C_{05}}{(C+C_{05})\times 1/2}\times 100 \quad (1)$$

where C is the methane total column and C_{05} the methane total column at the time 2005.0 ~~as~~ derived from the linear component of the Fourier series (Gardiner et al., 2008) fitted to the time series ~~(see Sect. 3)~~. The reference columns are given for each station in Table 3. It should be mentioned that the Toronto methane columns from 2008 to early 2009 present a systematic error due to an unknown instrument artifact. The dataset was corrected by adding a constant offset to the data over that period. To do this, a linear regression was first performed on the full dataset (20 June 2002 to 13 December 2014) excluding the biased data, and then another linear fit was performed only on the biased data (1 January 2008 to 19 March 2009) using the same fixed slope. The difference between the two intercepts gives a constant offset of molecules cm^{-2} that was added to the biased data.

In order to investigate~~characterize~~ on the possible impact of the choice of the microwindows and spectroscopy on the retrieved methane, each strategy has been tested over a set of spectra recorded at the Jungfraujoch station (3068 spectra recorded between 01-01-2005 and 12-31-2012). Mean fractional differences between the strategies described in Table 2 have been computed to quantify a potential absolute bias in terms of total columns and changes over the 2005-2012 time period with the inversion strategy optimized for the Jungfraujoch observations set as a reference. Mean fractional differences are defined as the difference between two datasets divided by their arithmetic average and expressed in percent (see Eq. 2 in Strong et al., 2008). This results in an averaged bias between total columns of 0.9 ± 0.5 % but no bias between their respective trends since 2005 is observed (reference values associated with the JFJ strategy in Table 2 are a mean total column of $2.4121 \pm 0.0055 \times 10^{19}$ molecules cm^{-2} and a mean annual change of 0.22 ± 0.04 % $year^{-1}$ with respect to 2005.0).

2.2.2 Information content

Due to the previously mentioned unresolved discrepancies associated with methane spectroscopic parameters, it has been established within the NDACC Infrared Working Group that the regularization strength of the methane retrieval strategy should

Mis en forme : Français (Belgique)
Mis en forme : Français (Belgique)
Code de champ modifié
Mis en forme : Français (Belgique)
Mis en forme : Français (Belgique)
Code de champ modifié
Mis en forme : Français (Belgique)
Code de champ modifié
Mis en forme : Surlignage
Mis en forme : Espace Avant : 6 pt, Après : 6 pt
Mis en forme : Surlignage
Mis en forme : Surlignage
Mis en forme : Surlignage
Mis en forme : Surlignage
Mis en forme : Surlignage
Mis en forme : Surlignage
Mis en forme : Surlignage
Mis en forme : Surlignage
Mis en forme : Surlignage
Mis en forme : Surlignage
Mis en forme : Police :Cambria Math, Italique, Surlignage
Mis en forme : Surlignage
Mis en forme : Indice, Surlignage
Mis en forme : Surlignage
Mis en forme : Surlignage
Mis en forme : Surlignage

be optimized so that the Degrees of Freedom For Signal (DOFS) is limited to a value of approximately 2 (Sussmann et al., 2011). As a consequence, the typical information content of NDACC methane retrievals will allow us to retrieve tropospheric and stratospheric columns, as displayed in Fig. 3. Indeed, the first eigenvector (in green) and its associated eigenvalue (typically close to 1) show that the corresponding information is mainly coming from the retrieval (> 99 %), allowing us to retrieve a partial column ranging from the surface up until 30 km. In addition, the second eigenvector allows for a finer vertical resolution with two supplementary partial columns with typically around 16 % of a priori dependence: (i) a tropospheric column (typically from the surface to the vicinity of the mean tropopause height of the station) along with (ii) a stratospheric column (from around the mean tropopause height to 30 km). In terms of error budget, extensive error analysis has been performed by Sepúlveda et al. (2014) and Sussmann et al. (2011). It has been determined that spectroscopic parameters almost exclusively determine the systematic error and amounts to ~2.5 % while statistical errors, dominated by baseline uncertainties and measurement noise, sum up to ~1 % (Sepúlveda et al., 2014).

As illustrated in Fig. 3, the information content of our retrievals sets the upper and lower limit of respectively our tropospheric and stratospheric column at the vicinity of the mean tropopause height of the station. Therefore, the typical vertical sensitivity range of our retrieval restricts our definition of a purely tropospheric component. Indeed, our tropospheric column as previously defined may potentially include a stratospheric contribution due to tropopause altitude variation, hence preventing the sampling of the free tropospheric column in some cases (Sepúlveda et al., 2014).

3. Methane changes since 2005

We characterize the global increase of methane total column from ten NDACC stations since 2005 and over 10 years' worth of observations, with a mean annual growth ranging from 0.26 ± 0.02 (Wollongong, 2-sigma level of uncertainty) to 0.39 ± 0.09 % year^{-1} (Toronto). Observational methane time series anomaly and their changes (along with their associated uncertainties) since 2005.0, illustrated in green in Fig. 4 and detailed in Table 3, have been analyzed for all ten sites using the statistical bootstrap resampling tool accounting for a linear component and a Fourier series taking into account the intra-annual variability of the dataset (Gardiner et al., 2008). As in Mahieu et al. (2014), the order of the Fourier series is adapted to each dataset depending on their sampling, i.e. limiting the order for the polar sites for which only a partial representation of the seasonality is available. Anomalies of methane total column time series, illustrated in Fig. 4, have been computed using the methane total column computed by the linear component of the statistical bootstrap tool on 1 January 2005, as a reference. Table 3 shows trends of methane total column computed from FTIR observations over the 2005-2014 and 2005-2012 time periods as well as from a tagged GEOS-Chem simulation between 2005 and 2012. The latter is further discussed in Sect. 3.1.2.

On a regional scale, we compared our results with annual changes of methane as computed over the 2005-2014 time period from surface GC-MD observations (Gas Chromatography – Multi Detector) performed in the framework of the AGAGE program (Advanced Global Atmospheric Gases Experiment, Prinn et al., 2000) and from in situ surface measurements performed in the framework of the NOAA (National Oceanic and Atmospheric Administration) ESRL (Earth System Research Laboratory) carbon cycle air sampling network (Dlugokencky et al., 2015). Five representative observation sites have been considered : Alert (Nunavut, Canada, 82.45 °N, -62.51 °E, 200.00 m a.s.l., Dlugokencky et al., 2015), Mace Head (Ireland, 53.33 °N, -9.90 °E, 5.00 m a.s.l., Prinn et al., 2000), Izaña (28.29 °N, 16.48 °W, 2372.90 m a.s.l., Dlugokencky et al., 2015), Cape Grim (Australia, 40.68 °S, 144.69 °E, 94.00 m a.s.l., Prinn et al., 2000), and Halley (United Kingdom, 75.61 °S, 26.21 °W, 30.00 m a.s.l., Dlugokencky et al., 2015).

Firstly, in situ measurements collected at Alert, representative of the northern polar region, show an increase of methane of 0.29 ± 0.02 % year^{-1} (or 5.40 ± 0.41 ppb year^{-1}) since 2006 which is in agreement with our FTIR observations at Eureka with a mean annual change of 0.28 ± 0.05 % year^{-1}. For the northern mid-latitudes, we find an agreement between changes of methane as computed from surface measurements at Mace Head with an increase of 0.30 ± 0.02 % year^{-1} (or 5.58 ± 0.32 ppb year^{-1}) and from our FTIR observations. Indeed, we observe consistent increases of methane of 0.32 ± 0.03, 0.27 ± 0.03, and 0.29 ± 0.08 % year^{-1} since 2005 at Zugspitze, Jungfraujoch and Toronto, respectively. Comparisons between changes of methane from FTIR and in situ surface measurements have also been performed for the Izaña station and show a close to statistical agreement with respectively a mean annual increase of 0.33 ± 0.01 and 0.28 ± 0.02 % year^{-1}. In the southern hemisphere, AGAGE GC-MD measurements of methane at Cape Grim, representative of the mid-latitudes, shows a mean annual increase of 0.31 ± 0.01 % year^{-1} (or 5.40 ± 0.16 ppb year^{-1}) which is in agreement with FTIR changes at Lauder of 0.29 ± 0.03 % year^{-1}. However, we should note the slightly larger mean annual changes of methane of Cape Grim in situ observations with respect to Wollongong FTIR measurements. Indeed, it needs to be mentioned that FTIR measurements before the instrument change in 2007 (Bomem DA8 vs Bruker IFS 125HR, see Table 1) show noisier results. These noisier observations at the beginning of the time period under investigation may affect the relatively small annual changes of methane overall. As a result, the 2005-2007 time series shows no changes of methane while the 2007-2014 time period shows a mean annual change of 0.32 ± 0.03 % year^{-1} (or 11.94 ± 1.03 x 10^{16} molecules cm^{-2} year^{-1}) with respect to 2007.0, which is in agreement with both Lauder FTIR and Cape Grim GC-MD methane changes since 2005. Finally, we computed a mean annual change of methane of 0.32 ± 0.01 % year^{-1} (or 5.45 ± 0.14 ppb year^{-1}) from in situ surface measurements performed at Halley which is in good agreement with the mean annual change of methane computed from FTIR Arrival Heights retrievals that amounts at 0.32 ± 0.07 % year^{-1}.

In summary, we globally observe from NDACC FTIR measurements an average annual change of methane of 0.31 ± 0.03 % year^{-1} (averaged over ten stations, 2-sigma level of uncertainty) which is in agreement with a mean annual change of 0.31 ± 0.01 % year^{-1} (or 5.51 ± 0.17 ppb year^{-1}), as computed from the monthly global means of baseline data derived from AGAGE measurements (Prinn et al., 2000).

In addition, analysis of tropospheric and stratospheric partial columns changes show tropospheric mean annual changes of methane statistically in agreement (at the 2-σ level) with changes of total column over the 2005-2014 time period. Mean annual changes from the Atmospheric Chemistry Experiment-Fourier Transform Spectrometer methane research product (ACE-FTS, Bernath et al., 2005) have also been examined. For consistent comparison, ACE-FTS stratospheric columns of methane have been defined the same way than the stratospheric FTIR product, i.e. from the average tropopause height of the station to 30 km. Changes of stratospheric methane according to ACE-FTS retrievals are statistically in agreement with our NDACC FTIR changes of stratospheric columns and show small to non-significant changes of methane in the stratosphere. Indeed, changes of stratospheric methane according to the ACE-FTS methane research product (Buzan et al., 2016) are not significant and amount to -0.12 ± 0.13 % year^{-1} for the northern high-latitudes, 0.10 ± 0.30 for northern mid-latitudes, 0.08 ± 0.24 for the tropical region, -0.10 ± 0.31 for the southern mid-latitudes, and -0.04 ± 0.14 % year^{-1} for the southern high-latitudes.

3.1 GEOS-Chem tagged simulation

GEOS-Chem (version 9-02: http://acmg.seas.harvard.edu/geos/doc/archive/man.v9-02/index.html, Turner et al., 2015) is a global 3-D CTM capable of simulating global trace gas and aerosol distributions. GEOS-Chem is driven here by assimilated meteorological fields from the Goddard Earth Observing System version 5 (GEOS-5) of the NASA Global Modeling

Code de champ modifié

Assimilation Office (GMAO). The GEOS-5 meteorological data have a temporal frequency of 6 h (3 h for mixing depths and surface properties) and are at a native horizontal resolution of 0.5°x0.667° with 72 hybrid pressure-σ levels describing the atmosphere from the surface up to 0.01 hPa. In the framework of this study, the GEOS-5 fields are degraded for model input to a 2°x2.5° horizontal resolution and 47 vertical levels by collapsing levels above ~80 hPa. GEOS-Chem has been extensively evaluated in the past (van Donkelaar et al., 2012; Park et al., 2006, 2004, Zhang et al., 2011, 2012). These studies show a good simulation of global transport with no apparent biases.

Code de champ modifié

Emissions for the GEOS-Chem simulations are from the EDGAR v4.2 anthropogenic methane inventory (European Commission, 2011), the wetland model from Kaplan (2002) as implemented by Pickett-Heaps et al. (2011), the GFED3 biomass burning inventory (van der Werf et al., 2010), a termite inventory and soil absorption from Fung et al. (1991), and a biofuel inventory from Yevich and Logan (2003). Wetland emissions vary with local temperature, inundation, and snow cover. Open fire emissions are specified with 8 hr temporal resolution. Other emissions are assumed aseasonal. Methane loss is mainly by reaction with the OH radical. We use a 3-D archive of monthly average OH concentrations from Park et al. (2004). The resulting atmospheric lifetime of methane is 8.9 years, consistent with the observational constraint of 9.1 ± 0.9 years (Prather et al., 2012).

The GEOS-Chem model output presented here covers the period January 2005-December 2012, for which the GEOS-5 meteorological fields are available. We use for this simulation, the best emission inventories available as implemented in version 9-02 of the model and rely on the spatial and temporal distributions of emissions. This tagged simulation includes 11 tracers : one tracer for the soil absorption sink (sa) and ten tracers for sources: gas and oil (ga), coal (co), livestock (li), waste management (wa), biofuels (bf), rice cultivation (ri), biomass burning (bb), wetlands (wl), other natural emissions (on) and other anthropogenic (oa) emissions. We have used a one-year run for spin-up from January 2004 to December 2004, restarted 70 times for initialization of the tracer concentrations. The model outputs consist of methane mixing ratio profiles saved at a 3-h time frequency and at the closest pixel to each NDACC station. To account for the vertical resolution and sensitivity of the FTIR retrievals, the individual concentration profiles simulated by GEOS-Chem are interpolated onto the FTIR vertical grid (see next section for description of regridding).

3.1.1 Data regridding and processing

In order to perform a proper comparison between the GEOS-Chem outputs and our NDACC FTIR observations we accounted for their respective spatial domains and used a conservative regridding scheme so that the total mass of the tracer is preserved (both locally and globally over the entire vertical profile). This was achieved using an algorithm similar to the one described in Sect. 3.1. of Langerock et al. (2015). To this end, time-dependent elevation coordinates are first calculated for the model outputs using grid-box heights data and providing topography data regridded onto the GEOS-Chem horizontal grid before conservative regridding.

The model outputs (source grid) are then regridded onto an observation-compliant destination grid through our conservative regridding scheme that includes a nearest-neighbor interpolation and a vertical regridding. The vertical destination grid corresponds to the retrieval grid adopted for each station. Regridded fields (tracer mixing-ratio) may have undefined values, for cells of the destination grid that do not overlap with the model source grid. For grid-cells that partially overlap the model grid, we apply a "mask tolerance", i.e., a relative overlapping volume threshold below which the value of the grid-cell will be set as undefined. This may introduce conservation errors, but since partially overlapping cells are likely to occur only at the top level of the model vertical grid, these errors can be neglected for species that usually have a low mixing-ratio at that level, such as methane.

To account for the vertical resolution and sensitivity of the FTIR retrievals, the individual concentration profiles simulated by GEOS-Chem are averaged into daily profiles (including day and night simulation) and smoothed according to:

$$\boldsymbol{x_{smooth}} = x_a + A(\boldsymbol{x_m} - \boldsymbol{x_a})\cancel{\boldsymbol{A} + \boldsymbol{x_a}} \qquad (1)$$

where A is the FTIR averaging kernels, x_m is the daily mean profile as simulated by the GEOS-Chem model regridded to the observation retrieval grid and x_a the FTIR a priori used in the retrieval according to the formalism of Rodgers [1990]. Averaging kernels are seasonal averages combining individual matrices from FTIR retrievals. Concerning the methane tracers, we constructed vertical a priori profiles for each of them by scaling the methane a priori employed for each station in order to smooth them as well. To this end, we determined for the ten sites the contribution of each tracer to the total methane on the basis of the mean budget simulated by the model over the 2005-2012 time period.

3.1.2 GEOS-Chem simulation vs NDACC FTIR observations

As we previously pointed out, since the information content of the FTIR retrievals prevents from retrieving a pure tropospheric component, we will focus on comparisons between FTIR and GEOS-Chem total columns. Due to the availability of the GEOS-5 meteorological fields and to ensure consistency, we limited our comparison of methane changes between FTIR observations and the GEOS-Chem simulation over the 2005-2012 time period. It is however worth mentioning that methane changes as observed by our FTIR observations are in agreement for all ten stations (see Fig. 4 and Table 3) between both time periods, i.e. 2005-2012 and 2005-2014.

Firstly, comparisons between FTIR observations and the smoothed GEOS-Chem simulation over the 2005-2012 time period have been performed for each NDACC station, for days when observations are available. Both time series are illustrated on Fig. 5 as anomalies with respect to 2005.0 (see corresponding reference columns in Table 3). We report a good agreement between FTIR and GEOS-Chem methane with no systematic bias (see definition of mean fractional differences given in Sect. 2.2.1 and Eq. 2 in Strong et al., 2008), except for the Tsukuba, Lauder and Arrival Heights stations where GEOS-Chem shows a systematic bias of -3.2 ± 3.1 %, 2.3 ± 1.7 % and 4.8 ± 3.5 % (2~~1~~-sigma level of uncertainty), with their respective FTIR observations. Since we defined the methane anomaly at 0 % in 2005.0 (or 2006.0 for Eureka) for both our observations and the GEOS-Chem simulation, we consequently corrected this observed bias on Fig. 5. On the other hand, we observe a slight phase offset between FTIR and GEOS-Chem seasonal cycles for Izaña and Tsukuba. Indeed, GEOS-Chem simulates the maximum methane column 85 days ahead of FTIR measurements for Izaña while it shows a delay of 92 days with respect to the Tsukuba FTIR time series. It should however be pointed out that the seasonal cycle's amplitude is well reproduced by GEOS-Chem with a peak-to-peak amplitude of~~-~~ 5.0 ± 0.9 % for Tsukuba and of 3.6 ± 0.5 % for Izaña while the methane seasonal cycle from FTIR measurements shows a peak-to-peak amplitude of 5.9 ± 1.7 % and 4.3 ± 1.8 %, respectively.

Regarding the increase of methane as simulated by GEOS-Chem, the simulation indicates a mean annual increase ranging from 0.31 ± 0.03 to 0.43 ± 0.06 %/year and a globally averaged annual change of 0.35 ± 0.03 %/year with respect to 2005.0 (averaged over ten stations, 2-sigma level of uncertainty). Mean annual changes of total columns of methane between 2005 and 2012 for both FTIR measurements and the GEOS-Chem simulation are illustrated on Fig. 4 in blue and orange respectively. In terms of methane increase, the model is in good agreement (within error bars) with the observations except for Jungfraujoch, Izaña and Wollongong where GEOS-Chem shows an overestimation of the methane increase.

We first discuss the possible causes of the slight trend discrepancy between FTIR observations at Jungfraujoch and Zugspitze as well as with GEOS-Chem for both stations~~Jungfraujoch~~. Indeed, despite their proximity (~250 km apart) and their respective altitude of 3580 m and 2954 m, both Alpine sites show distinct influences from local thermal induced vertical transport. At mountain-~~-~~type sites, subsidence is predominant for anticyclonic weather conditions resulting in adiabatic warming and cloud dissipation. The clear sky and strong radiation conditions lead to the convective growth of the atmospheric boundary layer (ABL) that ~~and~~ induce thermal~~ly induced~~ injections of ABL air ~~can reach~~ to the high-altitude observation~~of those~~ sites (Collaud Coen et al., 2011; Henne et al., 2005; Nyeki et al., 2000). In addition, mountain venting induced by higher temperatures allows the transport of ABL air to the free troposphere occurring often in summer~~-~~(between April and Auguts; Henne et al., 2005; Kreipl, 2006)~~(between April and August; Henne et al., 2005)~~. While the~~At~~ Jungfraujoch site is a remote site mostly influenced by free tropospheric airmasses with incursions of ABL airmasses during 50% of the sping and summer time (Collaud Coen et al., 2011; Henne et al., 2005, 2010; Okamoto and Tanimoto, 2016; Zellweger et al., 2000, 2003), the Zugspitze site is more often influenced by the ABL (Henne et al., 2010). For summer, when the influence of the ABL is the largest, the observed changes are in very close agreement, with 0.25 ± 0.06 and 0.26 ± 0.09 %/year^{-1}, respectively. ~~the airmasses originating from the ABL amount to only 30% of the year (Collaud Coen et al., 2011). More specifically in summer, airmasses originate from the ABL 50% of the time (Collaud Coen et al., 2011). I~~Moreover, it has been established that vertical export of airmasses above mountainous terrain is presently poorly represented in global CTMs (Henne et al., 2004). ~~In addition,~~ M~~m~~ean annual changes of GEOS-Chem methane agree with the observations in~~for~~ summer, during the influence of the ABL, with 0.33 ± 0.04 and 0.27 ± 0.08 % year^{-1} for Jungfraujoch and Zugspitze respectively. ~~and winter measurements show that with respectively 0.25 ± 0.06 and 0.33 ± 0.04 % year^{-1}, FTIR measurements and GEOS-Chem agree in summer, during the influence of the ABL, while they do not agree in winter. Indeed, FTIR winter measurements show a non-significant mean annual winter change of 0.10 ± 0.13 % year^{-1} while~~ In contrast, GEOS-Chem shows a mean annual winter change of respectively 0.23 ± 0.11 and 0.19 ± 0.09 % year^{-1} which agrees with Zugspitze change observations but not with Jungfraujoch changes. Since FTIR measurements and GEOS-Chem methane changes comparisons show a disagreement ~~agree~~ on the methane changes during winter~~in summer~~ at Jungfraujoch, ~~when under the influence of the ABL,~~ this seasonal analysis of changes of methane at mountaineous observations sites~~Jungfraujoch~~ emphasizes the current poor representation of summer versus winter thermal convection of air masses from the boundary layer to the free troposphere by the model.

About Izaña, it is worth mentioning that the FTIR methane total column time series shows a smaller seasonal cycle. Indeed, the combination of no local emission sources in the vicinity of Izaña, good mixing of airmasses and a regular solar insolation associated with more constant OH amounts leads to a dampened seasonal cycle (Dlugokencky et al., 1994) at that site. Therefore, small annual changes of methane and smaller uncertainty on the mean annual change computed by the bootstrap method complicates the agreement between the FTIR and GEOS-Chem methane changes. However, as mentioned above, it should be pointed out that the amplitude of this smaller seasonal cycle is well reproduced by the GEOS-Chem simulation.

About Wollongong, as already pointed out, noisier observations at the beginning of the period of interest may affect the relatively small annual changes of methane overall. In addition, one should not forget that sites such as Izaña or Wollongong can be challenging sites for models to reproduce due to the topography and land-sea contrast (Kulawik et al., 2015).

3.1.3. Tagged simulation analysis

The GEOS-Chem tagged simulation, which provides the contribution of each tracer to the total methane simulated, enables us to quantify and express the contribution of each tracer to the global methane increase. In order to do so, we considered year-to-year relative changes according to the following equation:

Mis en forme : Français (Belgique)

Code de champ modifié

Mis en forme : Français (Belgique)

Mis en forme : Exposant

Mis en forme : Exposant

$$YC\ (in\ \%) = (\mu_n - \mu_{n-1})/\mu_{tot,n-1} \qquad (2)$$

where μ_n is the annual mean of the simulated methane for the year n. The year-to-year relative changes are computed so that when we assume a relative change of a tracer for the year n, it is expressed with respect to the previous year (n-1) using $\mu_{tot,\ n-1}$ the annual mean of the simulated cumulative methane for the year (n-1) as a reference. Average of the individual relative year-to-year changes of total methane are in agreement with the mean annual change computed by the bootstrap method within error bars (2-sigma level uncertainty, Table 3). Therefore, the considered relative year-to-year changes of each tracer and for each site are illustrated on Fig. 6. The first three contributors to the annual methane change over the 2005-2012 time period are displayed for each site in Table B~~A.~~1 (see Appendix B~~A~~) along with the cumulative relative increase for the whole 2005-2012 time period.

On a global scale, we observe from the tracer analysis as simulated by GEOS-Chem that natural emission sources such as emissions from wetlands and biomass burning fluctuate inter-annually and thus are the dominant contributors to the interannual variability in methane surface emissions. This is in agreement with the finding of Bousquet et al. (2011), that fluctuations in wetland emissions are the dominant contribution to interannual variability in surface emissions, explaining 70% of the global emission anomalies over the past two decades, while biomass burning contributes only 15%. Regarding wetlands emissions, the simulation shows a mean net increase of methane in 2006 of +0.30 % (mean value over all sites) attributed to the tracer. In 2007-2008, GEOS-Chem simulates a stabilization of methane in the atmosphere due to the reduction of wetland emissions. Indeed, we observe either a slightly negative change in wetlands methane of -0.08 ± 0.07 % and of -0.08 ± 0.04 % respectively in 2008 and 2009 (mean values over all sites) or a minor increase not larger than 0.07 % in Arrival Heights (in 2009), in Tsukuba (in 2008) and in the high-latitude sites (i.e. Eureka and Kiruna in 2008 and 2009). On the other hand, the biomass burning tracer globally shows a net increase of 0.10 ± 0.01 % in 2007 likely due to the major fire season in tropical South America (Bloom et al., 2015) and a net decrease of -0.09 ± 0.01 % in 2009 and of -0.07 ± 0.01 % in 2012 with respect to the previous year. On the sink side, we find a negative phase between the relative year-to-year changes of the soil absorption tracer and the total methane simulated by GEOS-Chem except for Izaña where it remains positive over the time period studied.

On a local scale, we observe a slowdown of the increase in 2010 at mid-latitude sites (i.e. Zugspitze, Jungfraujoch, Toronto) and in 2011 at Tsukuba and at the high-latitude sites of Eureka and Kiruna. Following this stabilization phase, European sites find a substantial increase of more than 1.15 % in 2011 with respect to the previous year which is mainly due to an anomaly of wetlands emissions (+ 0.38 %) but also as a result of a relative increase of +0.21 % and +0.17 % of emissions from livestock and coal, respectively. The Izaña site presents the most regular increase mainly due to a smaller variability over the whole time period (seasonal cycle of Izaña previously discussed in Sect. 3.1.2.). In contrast, methane over Arrival Heights shows high variability from one year to another, which illustrates how dynamically sensitive the polar air is to transport from lower latitudes (Strahan et al., 2015).

Finally, regarding anthropogenic emissions, with positive year-to-year changes during the whole 2005-2012 time period, the coal and the gas and oil emissions are both regularly increasing through time. According to the GEOS-Chem tagged simulation, they both rank as the most important anthropogenic contributors to methane changes for all stations (see Appendix A) and thus substantially contribute to the total methane increase. In fact, the coal and the gas and oil tracers respectively comprise a third (32 %) and almost a fifth (18 %) of the cumulative increase of methane over the 2005-2012 time period while their respective emissions are responsible for only 7.5 and 12.5 % of the methane budget. As a comparison, the cumulative increase of methane emitted from wetlands, amounts to 16 % of the total increase since 2005 while wetland emissions makes up 34 % of the methane budget.

4. Discussion and conclusions

The cause of the methane increase since the mid-2000s has been often discussed and has still not been completely resolved (Aydin et al., 2011; Bloom et al., 2010; Dlugokencky et al., 2009; Hausmann et al., 2016; Kirschke et al., 2013; Nisbet et al., 2014; Rigby et al., 2008; Ringeval et al., 2010; Schaefer et al., 2016; Sussmann et al., 2012). On the sink side, Rigby et al. (2008) identified a decrease of OH radicals with a large uncertainty (− 4 ± 14 %) from 2006 to 2007 while Montzka et al. (2011) found a small drop of ~1 % year^{-1}, which might have contributed to the enhanced methane in the atmosphere. On the other hand, Bousquet et al. (2011) reported that the changes in OH remain small (<1% over the 2006-2008 time period). Nevertheless, observations of small inter-annual variations are in agreement with the understanding that perturbations in the atmospheric composition generally buffer the global OH concentrations (Dentener, 2003; Montzka et al., 2011).

The small to non-significant changes of methane in the stratosphere, as reported from analysis of the ACE-FTS methane research product, confirm that the increase of methane takes place in the troposphere. It is indeed driven by increasing sources emitted from the ground (Bousquet et al., 2011; Nisbet et al., 2014; Rigby et al., 2008), affecting primarily its tropospheric abundance and justifying the need for a source-oriented analysis of this recent increase.

Our analysis of the GEOS-Chem tagged simulation determines that secondary contributors to the global budget of methane such as coal mining, gas and oil transport and exploitation, have played a major role in the increase of atmospheric methane observed since 2005. However, while the simulation we used comprises the best emission inventories available so far, it has its own limitations. Firstly, Schwietzke et al. (2014), Bergamaschi et al. (2013) and Bruhwiler et al. (2014) reported that the EDGAR v4.2 emission inventory overestimates the recent emission growth in Asia. Indeed, Turner et al. (2015) reported from a global GOSAT (Greenhouse gases Observing SATellite) inversion that Chinese methane emissions from coal mining are too large by a factor of 2. Other regional discrepancies between the EDGAR v4.2 inventory and the GOSAT inversion such as an increase in wetland emissions in South America and an increase in rice emissions in Southeast Asia, have been pointed out by Turner et al. (2015) as well. On the other hand, it has been showed that the current emissions inventories, including EDGAR v4.2, underestimate the emissions of methane associated with the gas and oil use and exploitation, as well as livestock emissions (Franco et al., 2015, 2016, Turner et al., 2015, 2016). Furthermore, Lyon et al. (2016) pointed out that emissions from oil and gas well pads may be missing from most bottom-up emission inventories. The problem of the source identification clearly resides in the need for a better characterization of anthropogenic emissions and especially in emissions of methane from the oil and gas and livestock sectors.

Concerning the oil and gas emissions, ethane has shown a sharp increase since 2009 of ~5 % year^{-1} at mid-latitudes and of ~3 % year^{-1} at remote sites (Franco et al., 2016) which is attributed to the recent massive growth of oil and gas exploitation in the North American continent, with the geographical origin of these additional emissions confirmed by Helmig et al. (2016). Since ethane shares an anthropogenic source of methane : the production, transport and use of natural gas and the leakage associated to it (at 62 %; Logan et al., 1981; Rudolph, 1995), Franco et al. (2016) were able to estimate an increase of oil and gas methane emissions ranging from 20 Tg year^{-1} in 2008 to 35 Tg year^{-1} in 2014, using the C_2H_6/CH_4 ratio derived from GOSAT measurements as a proxy, confirming the influence of fossil fuel and gas production emissions impact on the observed methane increase. Moreover, Hausmann et al. (2016) reported an oil and gas contribution to the renewed methane in Zugspitze of 39 % over the 2007-2014 time period based on C_2H_6/CH_4 ratio derived from an atmospheric two-box model. However, as Kort et al. (2016) and Peischl et al. (2016) pointed out, the variability in the C_2H_6/CH_4 ratio associated to oil and gas production needs to be taken into account in a more rigorous manner as the strength of the C_2H_6/CH_4 relationship strongly depends on the studied region and/or production basin.

Code de champ modifié

Code de champ modifié

Mis en forme : Anglais (États-Unis)

Mis en forme : Anglais (États-Unis)

Code de champ modifié

Code de champ modifié

Mis en forme : Anglais (États-Unis)

Mis en forme : Anglais (États-Unis)

In conclusion, we report changes of atmospheric methane between 2005 and 2014 from FTIR measurements performed at 10 ground-based NDACC observation sites for the first time. From the ten NDACC methane time series, we computed a mean global annual increase of total column methane of 0.31 ± 0.03 % year^{-1} (averaged over ten stations, 2-sigma level of uncertainty), using 2005.0 as reference, which is consistent with methane changes computed from in situ measurements. From the GEOS-Chem tagged simulation, accounting for 11 tracers (10 emission sources and one sink) and covering the 2005-2012 time period, we computed a mean annual change of methane of 0.35 ± 0.03 % year^{-1} since 2005, which is globally in good agreement with the FTIR mean annual changes. In addition, we presented a detailed analysis of the GEOS-Chem tracer changes on both global and local scales over the 2005-2012 time period. To this end, we considered relative year-to-year changes in order to quantify the contribution of each tracer to the global methane change since 2005. According to the GEOS-Chem tagged simulation, wetland methane contributes mostly to the interannual variability while sources that contribute the most to the observed increase of methane since 2005 are mainly anthropogenic and are coal mining, gas and oil exploitation, and livestock (from largest to smallest contribution). While we showed that GEOS-Chem agrees with our observations and consequently with in situ measurements, the repartition between the different sources of methane would greatly benefit from an improvement of the global emission inventories. As an example, Turner et al. (2015) suggested that EDGAR v4.2 underestimates the US oil and gas and livestock emissions while overestimating methane emissions associated to coal mining. From the emission source shared by both ethane and methane and from various ethane studies, it is clear that further attention has to be given to improved anthropogenic methane inventories, such as emission inventories associated with fossil fuel and natural gas production. This is essential in a context of the energy transition that includes the development of shale gas exploitation.

Finally, it is worth mentioning that Schaefer et al. (2016) argue with the fact that thermogenic emissions of methane are responsible for the renewed increase of methane during the mid-2000s. Indeed, from methane isotopologues observations and a one-box model deriving global emission strength and isotopic source signature, Schaefer et al. reports that the recent methane increase is predominantly due to biogenic emission sources such as agriculture and climate-sensitive natural emissions. These results contrast with the context of a booming natural gas production and the resumption of coal mining in Asia. However, it is also worth noting that the $^{13}C/^{12}C$ and D/H ratio of atmospheric methane show distinctive isotope signature depending on the source type (Bergamaschi, 1997; Bergamaschi et al., 1998; Quay et al., 1999; Snover et al., 2000; Whiticar and Schaefer, 2007). In the same way, isotopic fractionation occurs during sink processes with specific ratio depending on the removal pathway (Gierczak et al., 1997; Irion et al., 1996; Saueressig et al., 2001; Snover and Quay, 2000; Tyler et al., 2000). Therefore, the under-exploited analysis of the recent methane increase through trend analysis of methane isotopologues, such as $^{13}CH_4$ and CH_3D, is an innovative way of addressing the question of the source(s) responsible for the recent methane increase.

Code de champ modifié

Code de champ modifié

Acknowledgments

Most of the data used in this publication were obtained as part of the Network for the Detection of Atmospheric Composition Change (NDACC) and are publicly available (see http://www.ndacc.org). W. Bader has received frunding from the European Union’s Horizon 2020 research and innovation programme under the Marie Sklodowska-Curie grant agreement n° 704951. The University of Liège’s involvement has primarily been supported by the PRODEX and SSD programs funded by the Belgian Federal Science Policy Office (Belspo), Brussels. The Swiss GAW-CH program is further acknowledged. E. Mahieu is Research Associate with the F.R.S. – FNRS. The F.R.S. – FNRS further supported this work under Grant nº J.0093.15 and the Fédération Wallonie Bruxelles contributed to observational activities support. We thank O. Flock for the constant support during this research. We thank the International Foundation High Altitude Research Stations Jungfraujoch and Gornergrat

(HFSJG, Bern) for supporting the facilities needed to perform the observations. The Eureka measurements were made at the Polar Environment Atmospheric Research Laboratory (PEARL) by the Canadian Network for the Detection of Atmospheric Change (CANDAC), led by James R. Drummond and in part by the Canadian Arctic ACE/OSIRIS Validation Campaigns, led by Kaley A. Walker. They were supported by the AIF/NSRIT, CFI, CFCAS, CSA, EC, GOC-IPY, NSERC, NSTP, OIT, PCSP and ORF. Logistical and operational support at Eureka is provided by PEARL Site Manager Pierre Fogal, CANDAC operators, and the EC Weather Station. The Toronto measurements were made at the University of Toronto Atmospheric Observatory (TAO), which has been supported by CFCAS, ABB Bomem, CFI, CSA, EC, NSERC, ORDCF, PREA, and the University of Toronto. We also thank the CANDAC operators, and the many students, postdocs, and interns who have contributed to data acquisition at Eureka and Toronto. Analysis of the Eureka and Toronto NDACC data was supported by the CAFTON project, funded by the Canadian Space Agency's FAST Program. KIT, IMK-ASF would like to thank Uwe Raffalski and Peter Voelgel from the Swedish Institute of Space Physics (IRF) for their continuing support of the NDACC-FTIR site Kiruna. KIT, IMK-ASF would also like to thank E. Sepúlveda for the support in performing the FTIR measurements at Izaña. Garmisch work has been performed as part of the ESA GHG-cci project, and KIT, IMK-IFU acknowledge funding by the EC within the INGOS project. The Centre for Atmospheric Chemistry at the University of Wollongong involvement in this work is funded by Australian Research Council projects DP1601021598 and LE0668470. Measurements and analysis conducted at Lauder, New Zealand and Arrival Heights, Antarctica are supported by NIWA as part of its Government-funded, core research. We thank Antarctica New Zealand for logistical support for the measurements taken at Arrival Heights. A. J. Turner was supported by a Department of Energy (DOE) Computational Science Graduate Fellowship (CSGF). The ACE mission is supported primarily by the Canadian Space Agency. AGAGE is supported principally by NASA (USA) grants to MIT and SIO, and also by DECC (UK) and NOAA (USA) grants to Bristol University and by CSIRO and the Bureau of Meteorology (Australia). We further thank NOAA for providing in situ data for Alert, Izaña and Halley.

References

Aydin, M., Verhulst, K. R., Saltzman, E. S., Battle, M. O., Montzka, S. a, Blake, D. R., Tang, Q. and Prather, M. J.: Recent decreases in fossil-fuel emissions of ethane and methane derived from firn air., Nature, 476(7359), 198–201, doi:10.1038/nature10352, 2011.

Batchelor, R. L., Strong, K., Lindenmaier, R., Mittermeier, R. L., Fast, H., Drummond, J. R. and Fogal, P. F.: A New Bruker IFS 125HR FTIR Spectrometer for the Polar Environment Atmospheric Research Laboratory at Eureka, Nunavut, Canada: Measurements and Comparison with the Existing Bomem DA8 Spectrometer, J. Atmos. Ocean. Technol., 26(7), 1328–1340, doi:10.1175/2009JTECHA1215.1, 2009.

Bergamaschi, P.: Seasonal variations of stable hydrogen and carbon isotope ratios in methane from a Chinese rice paddy, J. Geophys. Res., 102(D21), 25383, doi:10.1029/97JD01664, 1997.

Bergamaschi, P., Lubina, C., Königstedt, R., Fischer, H., Veltkamp, A. C. and Zwaagstra, O.: Stable isotopic signatures (δ^{13}C, δD) of methane from European landfill sites, J. Geophys. Res., 103(D7), 8251–8265, 1998.

Bergamaschi, P., Houweling, S., Segers, A., Krol, M., Frankenberg, C., Scheepmaker, R. A., Dlugokencky, E., Wofsy, S. C., Kort, E. A., Sweeney, C., Schuck, T., Brenninkmeijer, C., Chen, H., Beck, V. and Gerbig, C.: Atmospheric CH_4 in the first decade of the 21st century: Inverse modeling analysis using SCIAMACHY satellite retrievals and NOAA surface measurements, J. Geophys. Res. Atmos., 118(13), 7350–7369, doi:10.1002/jgrd.50480, 2013.

Bloom, A. A., Palmer, P. I., Fraser, A., Reay, D. S. and Frankenberg, C.: Large-Scale Controls of Methanogenesis Inferred from Methane and Gravity Spaceborne Data, Science (80-.)., 327(5963), 322–325, doi:10.1126/science.1175176, 2010.

Bloom, A. A., Worden, J., Jiang, Z., Worden, H., Kurosu, T., Frankenberg, C. and Schimel, D.: Remote-sensing constraints on South America fire traits by Bayesian fusion of atmospheric and surface data, Geophys. Res. Lett., 42(4), 1268–1274, doi:10.1002/2014GL062584, 2015.

Bousquet, P., Ciais, P., Miller, J. B., Dlugokencky, E. J., Hauglustaine, D. A., Prigent, C., Van der Werf, G. R., Peylin, P., Brunke, E.-G., Carouge, C., Langenfelds, R. L., Lathiere, J., Papa, F., Ramonet, M., Schmidt, M., Steele, L. P., Tyler, S. C. and White, J.: Contribution of anthropogenic and natural sources to atmospheric methane variability, Nature, 443(7110), 439–443, 2006.

Bousquet, P., Ringeval, B., Pison, I., Dlugokencky, E. J., Brunke, E.-G., Carouge, C., Chevallier, F., Fortems-Cheiney, a., Frankenberg, C., Hauglustaine, D. a., Krummel, P. B., Langenfelds, R. L., Ramonet, M., Schmidt, M., Steele, L. P., Szopa, S., Yver, C., Viovy, N. and Ciais, P.: Source attribution of the changes in atmospheric methane for 2006–2008, Atmos. Chem. Phys., 11(8), 3689–3700, doi:10.5194/acp-11-3689-2011, 2011.

Bruhwiler, L., Dlugokencky, E., Masarie, K., Ishizawa, M., Andrews, A., Miller, J., Sweeney, C., Tans, P. and Worthy, D.: CarbonTracker-CH4: an assimilation system for estimating emissions of atmospheric methane, Atmos. Chem. Phys., 14(16), 8269–8293, doi:10.5194/acp-14-8269-2014, 2014.

Buzan, E. M., Beale, C. A., Boone, C. D. and Bernath, P. F.: Global stratospheric measurements of the isotopologues of methane from the Atmospheric Chemistry Experiment Fourier transform spectrometer, Atmos. Meas. Tech., 9(3), 1095–1111, doi:10.5194/amt-9-1095-2016, 2016.

Chen, Y.-H. and Prinn, R. G.: Estimation of atmospheric methane emissions between 1996 and 2001 using a three-dimensional global chemical transport model, J. Geophys. Res. Atmos., 111(D10), D10307, doi:10.1029/2005JD006058, 2006.

Collaud Coen, M., Weingartner, E., Furger, M., Nyeki, S., Prévôt, A. S. H., Steinbacher, M. and Baltensperger, U.: Aerosol climatology and planetary boundary influence at the Jungfraujoch analyzed by synoptic weather types, Atmos. Chem. Phys., 11(12), 5931–5944, doi:10.5194/acp-11-5931-2011, 2011.

Cox, C. J., Walden, V. P. and Rowe, P. M.: A comparison of the atmospheric conditions at Eureka, Canada, and Barrow, Alaska (2006-2008), J. Geophys. Res. Atmos., 117(D12), n/a-n/a, doi:10.1029/2011JD017164, 2012.

Dentener, F.: Interannual variability and trend of CH_4 lifetime as a measure for OH changes in the 1979–1993 time period, J. Geophys. Res., 108(D15), 4442, doi:10.1029/2002JD002916, 2003.

Dlugokencky, E. J.: Atmospheric methane levels off: Temporary pause or a new steady-state?, Geophys. Res. Lett., 30(19), 1992, doi:10.1029/2003GL018126, 2003.

Dlugokencky, E. J., Steele, L. P., Lang, P. M. and Masarie, K. A.: The growth rate and distribution of atmospheric methane, J. Geophys. Res., 99(D8), 17021, doi:10.1029/94JD01245, 1994.

Dlugokencky, E. J., Bruhwiler, L., White, J. W. C., Emmons, L. K., Novelli, P. C., Montzka, S. a., Masarie, K. a., Lang, P. M., Crotwell, a. M., Miller, J. B. and Gatti, L. V.: Observational constraints on recent increases in the atmospheric CH_4 burden, Geophys. Res. Lett., 36(18), L18803, doi:10.1029/2009GL039780, 2009.

Dlugokencky, E. J., Lang, P. M., Crotwell, a. M., Masarie, K. A., Crotwell, M. J. and Thoning, K. W.: Atmospheric methane dry air mole fractions from the NOAA ESRL carbon cycle cooperative global air sampling network, 1983-2015, , Version: 2015-08-03 [online] Available from: ftp://aftp.cmdl.noaa.gov/data/trace_gases/ch4/flask/surface/ (Accessed 9 May 2016), 2015.

van Donkelaar, A., Martin, R. V., Pasch, A. N., Szykman, J. J., Zhang, L., Wang, Y. X. and Chen, D.: Improving the Accuracy of Daily Satellite-Derived Ground-Level Fine Aerosol Concentration Estimates for North America, Environ. Sci. Technol., 46(21), 11971–11978, doi:10.1021/es3025319, 2012.

Dubravica, D., Birk, M., Hase, F., Loos, J., Palm, M., Sadeghi, A. and Wagner, G.: Improved spectroscopic parameters of methane in the MIR for atmospheric remote sensing, in High Resolution Molecular Spectroscopy 2013 meeting, Budapest, Hungary., 2013.

Duchatelet, P., Demoulin, P., Hase, F., Ruhnke, R., Feng, W., Chipperfield, M. P., Bernath, P. F., Boone, C. D., Walker, K. A. and Mahieu, E.: Hydrogen fluoride total and partial column time series above the Jungfraujoch from long-term FTIR measurements: Impact of the line-shape model, characterization of the error budget and seasonal cycle, and comparison with satellite and model data, J. Geophys. Res., 115(D22), doi:10.1029/2010JD014677, 2010.

Fogal, P. F., LeBlanc, L. M. and Drummond, J. R.: The Polar Environment Atmospheric Research Laboratory (PEARL): Sounding the Atmosphere at 80° North., Arctic, 66(3), 377–386, 2013.

Franco, B., Bader, W., Toon, G. C., Bray, C., Perrin, A., Fischer, E. V., Sudo, K., Boone, C. D., Bovy, B., Lejeune, B., Servais, C. and Mahieu, E.: Retrieval of ethane from ground-based FTIR solar spectra using improved spectroscopy: Recent burden increase above Jungfraujoch, J. Quant. Spectrosc. Radiat. Transf., 160, 36–49, doi:10.1016/j.jqsrt.2015.03.017, 2015.

Franco, B., Mahieu, E., Emmons, L. K., Tzompa-Sosa, Z. A., Fischer, E. V, Sudo, K., Bovy, B., Conway, S., Griffin, D., Hannigan, J. W., Strong, K. and Walker, K. A.: Evaluating ethane and methane emissions associated with the development of oil and natural gas extraction in North America, Environ. Res. Lett., 11(4), 44010, doi:10.1088/1748-9326/11/4/044010, 2016.

Frankenberg, C., Aben, I., Bergamaschi, P., Dlugokencky, E. J., van Hees, R., Houweling, S., van der Meer, P., Snel, R. and Tol, P.: Global column-averaged methane mixing ratios from 2003 to 2009 as derived from SCIAMACHY: Trends and variability, J. Geophys. Res., 116(D4), D04302, doi:10.1029/2010JD014849, 2011.

Fraser, A., Miller, C. C., Palmer, P. I., Deutscher, N. M., Jones, N. B. and Griffith, D. W. T.: The Australian methane budget: Interpreting surface and train-borne measurements using a chemistry transport model, J. Geophys. Res., 116(D20), D20306, doi:10.1029/2011JD015964, 2011.

Fung, I., John, J., Lerner, J., Matthews, E., Prather, M., Steele, L. P. and Fraser, P. J.: Three-dimensional model synthesis of the global methane cycle, J. Geophys. Res., 96(D7), 13033, doi:10.1029/91JD01247, 1991.

Gardiner, T., Forbes, A., de Mazière, M., Vigouroux, C., Mahieu, E., Demoulin, P., Velazco, V., Notholt, J., Blumenstock, T., Hase, F., Kramer, I., Sussmann, R., Stremme, W., Mellqvist, J., Strandberg, A., Ellingsen, K. and Gauss, M.: Trend analysis of greenhouse gases over Europe measured by a network of ground-based remote FTIR instruments, Atmos. Chem. Phys., 8(22), 6719–6727, doi:10.5194/acp-8-6719-2008, 2008.

Gierczak, T., Talukdar, R. K., Herndon, S. C., Vaghjiani, G. L. and Ravishankara, A. R.: Rate Coefficients for the Reactions of Hydroxyl Radicals with Methane and Deuterated Methanes, J. Phys. Chem. A, 101(17), 3125–3134, doi:10.1021/jp963892r, 1997.

Griffith, D. W. T., Jones, N. B. and Matthews, W. A.: Interhemispheric ratio and annual cycle of carbonyl sulfide (OCS) total column from ground-based solar FTIR spectra, J. Geophys. Res., 103(D7), 8447, doi:10.1029/97JD03462, 1998.

Grooß, J.-U. and Russell, J. M.: Technical note: A stratospheric climatology for O_3, H_2O, CH_4, NOx, HCl and HF derived from HALOE measurements, Atmos. Chem. Phys., 5(10), 2797–2807, doi:10.5194/acp-5-2797-2005, 2005.

Gunson, M. R., Abbas, M. M., Abrams, M. C., Allen, M., Brown, L. R., Brown, T. L., Chang, A. Y., Goldman, A., Irion, F. W., Lowes, L. L., Mahieu, E., Manney, G. L., Michelsen, H. A., Newchurch, M. J., Rinsland, C. P., Salawitch, R. J., Stiller, G. P., Toon, G. C., Yung, Y. L. and Zander, R.: The Atmospheric Trace Molecule Spectroscopy (ATMOS) Experiment: Deployment on the ATLAS space shuttle missions, Geophys. Res. Lett., 23(17), 2333–2336, doi:10.1029/96GL01569, 1996.

Hase, F.: Inversion von Spurengasprofilen aus hochaufgelösten bodengebundenen FTIR-Messungen in absorption, Karlsruhe, Germany., 2000.

Hase, F., Hannigan, J. W., Coffey, M. T., Goldman, A., Höpfner, M., Jones, N. B., Rinsland, C. P. and Wood, S. W.: Intercomparison of retrieval codes used for the analysis of high-resolution, ground-based FTIR measurements, J. Quant. Spectrosc. Radiat. Transf., 87(1), 25–52, doi:10.1016/j.jqsrt.2003.12.008, 2004.

Hausmann, P., Sussmann, R. and Smale, D.: Contribution of oil and natural gas production to renewed increase in atmospheric methane (2007–2014): top–down estimate from ethane and methane column observations, Atmos. Chem. Phys., 16(5), 3227–3244, doi:10.5194/acp-16-3227-2016, 2016.

Helmig, D., Rossabi, S., Hueber, J., Tans, P., Montzka, S. A., Masarie, K., Thoning, K., Plass-Duelmer, C., Claude, A., Carpenter, L. J., Lewis, A. C., Punjabi, S., Reimann, S., Vollmer, M. K., Steinbrecher, R., Hannigan, J. W., Emmons, L. K.,

Mis en forme : Allemand (Allemagne)

Mahieu, E., Franco, B., Smale, D. and Pozzer, A.: Reversal of global atmospheric ethane and propane trends largely due to US oil and natural gas production, Nat. Geosci., doi:10.1038/ngeo2721, 2016.

Henne, S., Furger, M., Nyeki, S., Steinbacher, M., Neininger, B., de Wekker, S. F. J., Dommen, J., Spichtinger, N., Stohl, A. and Prévôt, A. S. H.: Quantification of topographic venting of boundary layer air to the free troposphere, Atmos. Chem. Phys., 4(2), 497–509, doi:10.5194/acp-4-497-2004, 2004.

Henne, S., Furger, M. and Prévôt, A. H.: Climatology of Mountain Venting–Induced Elevated Moisture Layers in the Lee of the Alps, J. Appl. Meteorol., 44(5), 620–633, doi:10.1175/JAM2217.1, 2005.

Henne, S., Brunner, D., Folini, D., Solberg, S., Klausen, J. and Buchmann, B.: Assessment of parameters describing representativeness of air quality in-situ measurement sites, Atmos. Chem. Phys., 10(8), 3561–3581, doi:10.5194/acp-10-3561-2010, 2010.

Irion, F. W., Moyer, E. J., Gunson, M. R., Rinsland, C. P., Yung, Y. L., Michelsen, H. A., Salawitch, R. J., Chang, A. Y., Newchurch, M. J., Abbas, M. M., Abrams, M. C. and Zander, R.: Stratospheric observations of CH3D and HDO from ATMOS infrared solar spectra: Enrichments of deuterium in methane and implications for HD, Geophys. Res. Lett., 23(17), 2381–2384, doi:10.1029/96GL01402, 1996.

Kaplan, J. O.: Wetlands at the Last Glacial Maximum: Distribution and methane emissions, Geophys. Res. Lett., 29(6), 1079, doi:10.1029/2001GL013366, 2002.

Kirschke, S., Bousquet, P., Ciais, P., Saunois, M., Canadell, J. G., Dlugokencky, E. J., Bergamaschi, P., Bergmann, D., Blake, D. R., Bruhwiler, L., Cameron-Smith, P., Castaldi, S., Chevallier, F., Feng, L., Fraser, A., Heimann, M., Hodson, E. L., Houweling, S., Josse, B., Fraser, P. J., Krummel, P. B., Lamarque, J.-F., Langenfelds, R. L., Le Quéré, C., Naik, V., O'Doherty, S., Palmer, P. I., Pison, I., Plummer, D., Poulter, B., Prinn, R. G., Rigby, M., Ringeval, B., Santini, M., Schmidt, M., Shindell, D. T., Simpson, I. J., Spahni, R., Steele, L. P., Strode, S. a., Sudo, K., Szopa, S., van der Werf, G. R., Voulgarakis, A., van Weele, M., Weiss, R. F., Williams, J. E. and Zeng, G.: Three decades of global methane sources and sinks, Nat. Geosci., 6(10), 813–823, doi:10.1038/ngeo1955, 2013.

Kort, E. A., Smith, M. L., Murray, L. T., Gvakharia, A., Brandt, A. R., Peischl, J., Ryerson, T. B., Sweeney, C. and Travis, K.: Fugitive emissions from the Bakken shale illustrate role of shale production in global ethane shift, Geophys. Res. Lett., doi:10.1002/2016GL068703, 2016.

Kreipl, S.: Messung des Aerosoltransports am Alpennordrand mittels Laserradar (Lidar), Friedrich-Alexander-Universität Erlangen-Nürnberg, Erlangen-Nürnberg, Germany., 2006.

Kulawik, S. S., Wunch, D., O'Dell, C., Frankenberg, C., Reuter, M., Oda, T., Chevallier, F., Sherlock, V., Buchwitz, M., Osterman, G., Miller, C., Wennberg, P., Griffith, D. W. T., Morino, I., Dubey, M., Deutscher, N. M., Notholt, J., Hase, F., Warneke, T., Sussmann, R., Robinson, J., Strong, K., Schneider, M. and Wolf, J.: Consistent evaluation of GOSAT, SCIAMACHY, CarbonTracker, and MACC through comparisons to TCCON, Atmos. Meas. Tech. Discuss., 8(6), 6217–6277, doi:10.5194/amtd-8-6217-2015, 2015.

Langerock, B., De Mazière, M., Hendrick, F., Vigouroux, C., Desmet, F., Dils, B. and Niemeijer, S.: Description of algorithms for co-locating and comparing gridded model data with remote-sensing observations, Geosci. Model Dev., 8(3), 911–921, doi:10.5194/gmd-8-911-2015, 2015.

Lelieveld, J.: Stability of tropospheric hydroxyl chemistry, J. Geophys. Res., 107(D23), 4715, doi:10.1029/2002JD002272, 2002.

Logan, J. A., Prather, M. J., Wofsy, S. C. and McElroy, M. B.: Tropospheric chemistry: A global perspective, J. Geophys. Res., 86(C8), 7210, doi:10.1029/JC086iC08p07210, 1981.

Lyon, D. R., Alvarez, R. A., Zavala-Araiza, D., Brandt, A. R., Jackson, R. B. and Hamburg, S. P.: Aerial Surveys of Elevated Hydrocarbon Emissions from Oil and Gas Production Sites, Environ. Sci. Technol., 50(9), 4877–4886, doi:10.1021/acs.est.6b00705, 2016.

Mis en forme : Allemand (Allemagne)

Mahieu, E., Chipperfield, M. P., Notholt, J., Reddmann, T., Anderson, J., Bernath, P. F., Blumenstock, T., Coffey, M. T., Dhomse, S. S., Feng, W., Franco, B., Froidevaux, L., Griffith, D. W. T., Hannigan, J. W., Hase, F., Hossaini, R., Jones, N. B., Morino, I., Murata, I., Nakajima, H., Palm, M., Paton-Walsh, C., Russel III, J. M., Schneider, M., Servais, C., Smale, D. and Walker, K. A.: Recent Northern Hemisphere stratospheric HCl increase due to atmospheric circulation changes, Nature, 515(7525), 104–107, doi:10.1038/nature13857, 2014.

Montzka, S. A., Krol, M., Dlugokencky, E., Hall, B., Jockel, P. and Lelieveld, J.: Small Interannual Variability of Global Atmospheric Hydroxyl, Science (80-.)., 331(6013), 67–69, doi:10.1126/science.1197640, 2011.

Nisbet, E. G., Dlugokencky, E. J. and Bousquet, P.: Methane on the rise-again., Science, 343(6170), 493–5, doi:10.1126/science.1247828, 2014.

Nyeki, S., Kalberer, M., Colbeck, I., de Wekker, S. F. J., Furger, M., Gäggeler, H. W., Kossmann, M., Lugauer, M., Steyn, D., Weingartner, E., Wirth, M. and Baltensperger, U.: Convective boundary layer evolution to 4 km asl over High-Alpine terrain: airborne Lidar observations in the Alps, Geophys. Res. Lett., 27(5), 689–692, 2000.

Okamoto, S. and Tanimoto, H.: A review of atmospheric chemistry observations at mountain sites, Prog. Earth Planet. Sci., 3(1), 34, doi:10.1186/s40645-016-0109-2, 2016.

Park, R., Jacob, D., Kumar, N. and Yantosca, R.: Regional visibility statistics in the United States: Natural and transboundary pollution influences, and implications for the Regional Haze Rule, Atmos. Environ., 40(28), 5405–5423, doi:10.1016/j.atmosenv.2006.04.059, 2006.

Park, R. J., Jacob, D. J., Field, B. D., Yantosca, R. M. and Chin, M.: Natural and transboundary pollution influences on sulfate-nitrate-ammonium aerosols in the United States: Implications for policy, J. Geophys. Res., 109(D15), doi:10.1029/2003JD004473, 2004.

Peischl, J., Karion, A., Sweeney, C., Kort, E. A., Smith, M. L., Brandt, A. R., Yeskoo, T., Aikin, K. C., Conley, S. A., Gvakharia, A., Trainer, M., Wolter, S. and Ryerson, T. B.: Quantifying atmospheric methane emissions from oil and natural gas production in the Bakken shale region of North Dakota, J. Geophys. Res. Atmos., 121(10), 6101–6111, doi:10.1002/2015JD024631, 2016.

Pickett-Heaps, C. A., Jacob, D. J., Wecht, K. J., Kort, E. A., Wofsy, S. C., Diskin, G. S., Worthy, D. E. J., Kaplan, J. O., Bey, I. and Drevet, J.: Magnitude and seasonality of wetland methane emissions from the Hudson Bay Lowlands (Canada), Atmos. Chem. Phys., 11(8), 3773–3779, doi:10.5194/acp-11-3773-2011, 2011.

Pison, I., Ringeval, B., Bousquet, P., Prigent, C. and Papa, F.: Stable atmospheric methane in the 2000s: key-role of emissions from natural wetlands, Atmos. Chem. Phys., 13(23), 11609–11623, doi:10.5194/acp-13-11609-2013, 2013.

Prather, M. J., Holmes, C. D. and Hsu, J.: Reactive greenhouse gas scenarios: Systematic exploration of uncertainties and the role of atmospheric chemistry, Geophys. Res. Lett., 39(9), n/a-n/a, doi:10.1029/2012GL051440, 2012.

Prinn, R. G., Weiss, R. F., Fraser, P. J., Simmonds, P. G., Cunnold, D. M., Alyea, F. N., O'Doherty, S., Salameh, P., Miller, B. R., Huang, J., Wang, R. H. J., Hartley, D. E., Harth, C., Steele, L. P., Sturrock, G., Midgley, P. M. and McCulloch, A.: A history of chemically and radiatively important gases in air deduced from ALE/GAGE/AGAGE, J. Geophys. Res. Atmos., 105(D14), 17751–17792, doi:10.1029/2000JD900141, 2000.

Quay, P., Stutsman, J., Wilbur, D., Snover, A., Dlugokencky, E. and Brown, T.: The isotopic composition of atmospheric methane, Global Biogeochem. Cycles, 13(2), 445–461, doi:10.1029/1998GB900006, 1999.

Reimann, S.: Halogenated greenhouse gases at the Swiss High Alpine Site of Jungfraujoch (3580 m asl): Continuous measurements and their use for regional European source allocation, J. Geophys. Res., 109(D5), doi:10.1029/2003JD003923, 2004.

Rigby, M., Prinn, R. G., Fraser, P. J., Simmonds, P. G., Langenfelds, R. L., Huang, J., Cunnold, D. M., Steele, L. P., Krummel, P. B., Weiss, R. F., O'Doherty, S., Salameh, P. K., Wang, H. J., Harth, C. M., Mühle, J. and Porter, L. W.: Renewed growth of atmospheric methane, Geophys. Res. Lett., 35(22), L22805, doi:10.1029/2008GL036037, 2008.

Ringeval, B., de Noblet-Ducoudré, N., Ciais, P., Bousquet, P., Prigent, C., Papa, F. and Rossow, W. B.: An attempt to quantify the impact of changes in wetland extent on methane emissions on the seasonal and interannual time scales, Global Biogeochem. Cycles, 24(2), GB2003, doi:10.1029/2008GB003354, 2010.

Rinsland, C. P., Jones, N. B., Connor, B. J., Logan, J. A., Pougatchev, N. S., Goldman, A., Murcray, F. J., Stephen, T. M., Pine, A. S., Zander, R., Mahieu, E., Demoulin, P., Rinsland, C. P., Jones, N. B., Connor, B. J., Logan, J. A., Pougatchev, N. S., Goldman, A., Murcray, F. J., Stephen, T. M., Pine, A. S., Zander, R., Mahieu, E., Demoulin, P., Rinsland, C. P., Jones, N. B., Connor, B. J., Logan, J. A., Pougatchev, N. S., Goldman, A., Murcray, F. J., Stephen, T. M., Pine, A. S., Zander, R., Mahieu, E. and Demoulin, P.: Northern and southern hemisphere ground-based infrared spectroscopic measurements of tropospheric carbon monoxide and ethane, J. Geophys. Res., 103(D21), 28197–28217, doi:10.1029/98JD02515, 1998.

Rinsland, C. P., Goldman, A., Elkins, J. W., Chiou, L. S., Hannigan, J. W., Wood, S. W., Mahieu, E. and Zander, R.: Long-term trend of CH4 at northern mid-latitudes: Comparison between ground-based infrared solar and surface sampling measurements, J. Quant. Spectrosc. Radiat. Transf., 97(3), 457–466, doi:10.1016/j.jqsrt.2005.07.002, 2006.

Rodgers, C. D.: Characterization and error analysis of profiles retrieved from remote sounding measurements, J. Geophys. Res., 95(D5), 5587, 1990.

Rothman, L. S., Barbe, A., Chris Benner, D., Brown, L. R., Camy-Peyret, C., Carleer, M. R., Chance, K., Clerbaux, C., Dana, V., Devi, V. M., Fayt, A., Flaud, J.-M., Gamache, R. R., Goldman, A., Jacquemart, D., Jucks, K. W., Lafferty, W. J., Mandin, J.-Y., Massie, S. T., Nemtchinov, V., Newnham, D. A., Perrin, A., Rinsland, C. P., Schroeder, J., Smith, K. M., Smith, M. A. H., Tang, K., Toth, R. A., Vander Auwera, J., Varanasi, P. and Yoshino, K.: The HITRAN molecular spectroscopic database: edition of 2000 including updates through 2001, J. Quant. Spectrosc. Radiat. Transf., 82(1–4), 5–44, doi:10.1016/S0022-4073(03)00146-8, 2003.

Rothman, L. S., Gordon, I. E., Barbe, a., Benner, D. C., Bernath, P. F., Birk, M., Boudon, V., Brown, L. R., Campargue, a., Champion, J.-P., Chance, K., Coudert, L. H., Dana, V., Devi, V. M., Fally, S., Flaud, J.-M., Gamache, R. R., Goldman, a., Jacquemart, D., Kleiner, I., Lacome, N., Lafferty, W. J., Mandin, J.-Y., Massie, S. T., Mikhailenko, S. N., Miller, C. E., Moazzen-Ahmadi, N., Naumenko, O. V., Nikitin, a. V., Orphal, J., Perevalov, V. I., Perrin, a., Predoi-Cross, a., Rinsland, C. P., Rotger, M., Šimečková, M., Smith, M. a. H., Sung, K., Tashkun, S. a., Tennyson, J., Toth, R. a., Vandaele, a. C. and Vander Auwera, J.: The HITRAN 2008 molecular spectroscopic database, J. Quant. Spectrosc. Radiat. Transf., 110(9–10), 533–572, doi:10.1016/j.jqsrt.2009.02.013, 2009.

Rothman, L. S., Gordon, I. E., Babikov, Y., Barbe, A., Chris Benner, D., Bernath, P. F., Birk, M., Bizzocchi, L., Boudon, V., Brown, L. R., Campargue, A., Chance, K., Cohen, E. A., Coudert, L. H., Devi, V. M., Drouin, B. J., Fayt, A., Flaud, J.-M., Gamache, R. R., Harrison, J. J., Hartmann, J.-M., Hill, C., Hodges, J. T., Jacquemart, D., Jolly, A., Lamouroux, J., Le Roy, R. J., Li, G., Long, D. A., Lyulin, O. M., Mackie, C. J., Massie, S. T., Mikhailenko, S., Müller, H. S. P., Naumenko, O. V., Nikitin, A. V., Orphal, J., Perevalov, V., Perrin, A., Polovtseva, E. R., Richard, C., Smith, M. A. H., Starikova, E., Sung, K., Tashkun, S., Tennyson, J., Toon, G. C., Tyuterev, V. G. and Wagner, G.: The HITRAN2012 molecular spectroscopic database, J. Quant. Spectrosc. Radiat. Transf., 130, 4–50, doi:10.1016/j.jqsrt.2013.07.002, 2013.

Rudolph, J.: The tropospheric distribution and budget of ethane, J. Geophys. Res., 100(D6), 11369, doi:10.1029/95JD00693, 1995.

Saueressig, G., Crowley, J. N., Bergamaschi, P., Brühl, C., Brenninkmeijer, C. A. M. and Fischer, H.: Carbon 13 and D kinetic isotope effects in the reactions of CH_4 with $O(^1D)$ and OH: New laboratory measurements and their implications for the isotopic composition of stratospheric methane, J. Geophys. Res., 106(D19), 23127, doi:10.1029/2000JD000120, 2001.

Schaefer, H., Fletcher, S. E. M., Veidt, C., Lassey, K. R., Brailsford, G. W., Bromley, T. M., Dlugokencky, E. J., Michel, S. E., Miller, J. B., Levin, I., Lowe, D. C., Martin, R. J., Vaughn, B. H. and White, J. W. C.: A 21st-century shift from fossil-fuel to biogenic methane emissions indicated by 13CH4, Science (80-.)., 352(6281), 80–84, doi:10.1126/science.aad2705, 2016.

Schwietzke, S., Griffin, W. M., Matthews, H. S. and Bruhwiler, L. M. P.: Global Bottom-Up Fossil Fuel Fugitive Methane and Ethane Emissions Inventory for Atmospheric Modeling, ACS Sustain. Chem. Eng., 2(8), 1992–2001, doi:10.1021/sc500163h, 2014.

Sepúlveda, E., Schneider, M., Hase, F., García, O. E., Gomez-Pelaez, a., Dohe, S., Blumenstock, T. and Guerra, J. C.: Long-term validation of tropospheric column-averaged CH_4 mole fractions obtained by mid-infrared ground-based FTIR spectrometry, Atmos. Meas. Tech., 5(6), 1425–1441, doi:10.5194/amt-5-1425-2012, 2012.

Sepúlveda, E., Schneider, M., Hase, F., Barthlott, S., Dubravica, D., García, O. E., González, Y., Guerra, J. C., Gisi, M., Kohlhepp, R., Dohe, S., Blumenstock, T., Strong, K., Weaver, D., Palm, M., Sadeghi, A., Deutscher, N. M., Warneke, T., Notholt, J., Jones, N., Griffith, D. W. T., Smale, D., Brailsford, G. W. and Robinson, J.: Tropospheric CH4 signals as observed by NDACC FTIR at globally distributed sites and comparison to GAW surface in situ measurements, , 2337–2360, doi:10.5194/amt-7-2337-2014, 2014.

Simpson, I. J., Sulbaek Andersen, M. P., Meinardi, S., Bruhwiler, L., Blake, N. J., Helmig, D., Rowland, F. S. and Blake, D. R.: Long-term decline of global atmospheric ethane concentrations and implications for methane., Nature, 488(7412), 490–4, doi:10.1038/nature11342, 2012.

Snover, A. K. and Quay, P. D.: Hydrogen and carbon kinetic isotope effects during soil uptake of atmospheric methane, Global Biogeochem. Cycles, 14(1), 25–39, doi:10.1029/1999GB900089, 2000.

Snover, A. K., Quay, P. D. and Hao, W. M.: The D/H content of methane emitted from biomass burning, Global Biogeochem. Cycles, 14(1), 11–24, doi:10.1029/1999GB900075, 2000.

Solomon, S., Rosenlof, K. H., Portmann, R. W., Daniel, J. S., Davis, S. M., Sanford, T. J. and Plattner, G.-K.: Contributions of Stratospheric Water Vapor to Decadal Changes in the Rate of Global Warming, Science (80-.)., 327(5970), 1219–1223, doi:10.1126/science.1182488, 2010.

Spahni, R., Wania, R., Neef, L., van Weele, M., Pison, I., Bousquet, P., Frankenberg, C., Foster, P. N., Joos, F., Prentice, I. C. and van Velthoven, P.: Constraining global methane emissions and uptake by ecosystems, Biogeosciences, 8(6), 1643–1665, doi:10.5194/bg-8-1643-2011, 2011.

Stocker, T. F., Qin, D., Plattner, G.-K., Tignor, M., Allen, S. K., Boschung, J., Nauels, A., Xia, Y., Bex, V. and Midgley, P. M.: The Physical Science Basis. Contribution of Working Group I to the Fifth Assessment Report of the Intergovernmental Panel on Climate Change, Cambridge., Cambridge, United Kingdom and New York, NY, USA., 2013.

Strahan, S. E., Oman, L. D., Douglass, A. R. and Coy, L.: Modulation of Antarctic vortex composition by the quasi-biennial oscillation, Geophys. Res. Lett., 42(10), 4216–4223, doi:10.1002/2015GL063759, 2015.

Strong, K., Wolff, M. A., Kerzenmacher, T. E., Walker, K. A., Bernath, P. F., Blumenstock, T., Boone, C., Catoire, V., Coffey, M., De Mazière, M., Demoulin, P., Duchatelet, P., Dupuy, E., Hannigan, J., Höpfner, M., Glatthor, N., Griffith, D. W. T., Jin, J. J., Jones, N., Jucks, K., Kuellmann, H., Kuttippurath, J., Lambert, A., Mahieu, E., McConnell, J. C., Mellqvist, J., Mikuteit, S., Murtagh, D. P., Notholt, J., Piccolo, C., Raspollini, P., Ridolfi, M., Robert, C., Schneider, M., Schrems, O., Semeniuk, K., Senten, C., Stiller, G. P., Strandberg, A., Taylor, J., Tétard, C., Toohey, M., Urban, J., Warneke, T. and Wood, S.: Validation of ACE-FTS N2O measurements, Atmos. Chem. Phys., 8(16), 4759–4786, doi:10.5194/acp-8-4759-2008, 2008.

Sussmann, R. and Schäfer, K.: Infrared spectroscopy of tropospheric trace gases: combined analysis of horizontal and vertical column abundances, Appl. Opt., 36(3), 735, doi:10.1364/AO.36.000735, 1997.

Sussmann, R., Forster, F., Rettinger, M. and Jones, N.: Strategy for high-accuracy-and-precision retrieval of atmospheric methane from the mid-infrared FTIR network, Atmos. Meas. Tech., 4(9), 1943–1964, doi:10.5194/amt-4-1943-2011, 2011.

Sussmann, R., Forster, F., Rettinger, M. and Bousquet, P.: Renewed methane increase for five years (2007–2011) observed by solar FTIR spectrometry, Atmos. Chem. Phys., 12(11), 4885–4891, doi:10.5194/acp-12-4885-2012, 2012.

Tikhonov, A.: On the solution of incorrectly stated problems and a method of regularization, Dokl. Acad. Nauk SSSR, 151, 501–504, 1963.

Turner, A. J., Jacob, D. J., Wecht, K. J., Maasakkers, J. D., Lundgren, E., Andrews, A. E., Biraud, S. C., Boesch, H., Bowman,

K. W., Deutscher, N. M., Dubey, M. K., Griffith, D. W. T., Hase, F., Kuze, A., Notholt, J., Ohyama, H., Parker, R., Payne, V. H., Sussmann, R., Sweeney, C., Velazco, V. A., Warneke, T., Wennberg, P. O. and Wunch, D.: Estimating global and North American methane emissions with high spatial resolution using GOSAT satellite data, Atmos. Chem. Phys., 15(12), 7049–7069, doi:10.5194/acp-15-7049-2015, 2015.

Turner, A. J., Jacob, D. J., Benmergui, J., Wofsy, S. C., Maasakkers, J. D., Butz, A., Hasekamp, O., Biraud, S. C. and Dlugokencky, E.: A large increase in US methane emissions over the past decade inferred from satellite data and surface observations, Geophys. Res. Lett., n/a-n/a, doi:10.1002/2016GL067987, 2016.

Turner, J., Colwell, S. R., Marshall, G. J., Lachlan-Cope, T. A., Carleton, A. M., Jones, P. D., Lagun, V., Reid, P. A. and Iagovkina, S.: The SCAR READER Project: Toward a High-Quality Database of Mean Antarctic Meteorological Observations, J. Clim., 17(14), 2890–2898, doi:10.1175/1520-0442(2004)017<2890:TSRPTA>2.0.CO;2, 2004.

Tyler, S. C., Ajie, H. O., Rice, A. L., Cicerone, R. J. and Tuazon, E. C.: Experimentally determined kinetic isotope effects in the reaction of CH_4 with Cl: Implications for atmospheric CH_4, Geophys. Res. Lett., 27(12), 1715–1718, doi:10.1029/1999GL011168, 2000.

Wang, J. S., Logan, J. a., McElroy, M. B., Duncan, B. N., Megretskaia, I. a. and Yantosca, R. M.: A 3-D model analysis of the slowdown and interannual variability in the methane growth rate from 1988 to 1997, Global Biogeochem. Cycles, 18(3), GB3011, doi:10.1029/2003GB002180, 2004.

van der Werf, G. R., Randerson, J. T., Giglio, L., Collatz, G. J., Mu, M., Kasibhatla, P. S., Morton, D. C., DeFries, R. S., Jin, Y. and van Leeuwen, T. T.: Global fire emissions and the contribution of deforestation, savanna, forest, agricultural, and peat fires (1997–2009), Atmos. Chem. Phys., 10(23), 11707–11735, doi:10.5194/acp-10-11707-2010, 2010.

Whaley, C. H., Strong, K., Jones, D. B. A., Walker, T. W., Jiang, Z., Henze, D. K., Cooke, M. A., McLinden, C. A., Mittermeier, R. L., Pommier, M. and Fogal, P. F.: Toronto area ozone: Long-term measurements and modeled sources of poor air quality events, J. Geophys. Res. Atmos., 120(21), 11,368-11,390, doi:10.1002/2014JD022984, 2015.

Whiticar, M. and Schaefer, H.: Constraining past global tropospheric methane budgets with carbon and hydrogen isotope ratios in ice., Philos. Trans. A. Math. Phys. Eng. Sci., 365(1856), 1793–1828, doi:10.1098/rsta.2007.2048, 2007.

Wiacek, A., Taylor, J. R., Strong, K., Saari, R., Kerzenmacher, T. E., Jones, N. B. and Griffith, D. W. T.: Ground-based solar absorption FTIR spectroscopy: Characterization of retrievals and first results from a novel optical design instrument at a new NDACC complementary station, J. Atmos. Ocean. Technol., 24(3), 432–448, doi:10.1175/JTECH1962.1, 2007.

World Meteorological Organization: Greenhouse Gas Bulletin N°10, Geneva, Switzerland., 2014.

Yevich, R. and Logan, J. A.: An assessment of biofuel use and burning of agricultural waste in the developing world, Global Biogeochem. Cycles, 17(4), n/a-n/a, doi:10.1029/2002GB001952, 2003.

Zander, R., Mahieu, E., Demoulin, P., Duchatelet, P., Roland, G., Servais, C., Mazière, M. De, Reimann, S. and Rinsland, C. P.: Our changing atmosphere: Evidence based on long-term infrared solar observations at the Jungfraujoch since 1950, Sci. Total Environ., 391(2–3), 184–195, doi:10.1016/j.scitotenv.2007.10.018, 2008.

Zellweger, C., Ammann, M., Buchmann, B., Hofer, P., Lugauer, M., Rüttimann, R., Streit, N., Weingartner, E. and Baltensperger, U.: Summertime NO y speciation at the Jungfraujoch, 3580 m above sea level, Switzerland, J. Geophys. Res. Atmos., 105(D5), 6655–6667, doi:10.1029/1999JD901126, 2000.

Zellweger, C., Forrer, J., Hofer, P., Nyeki, S., Schwarzenbach, B., Weingartner, E., Ammann, M. and Baltensperger, U.: Partitioning of reactive nitrogen (NOy) and dependence on meteorological conditions in the lower free troposphere, Atmos. Chem. Phys., 3(3), 779–796, doi:10.5194/acp-3-779-2003, 2003.

Zhang, L., Jacob, D. J., Downey, N. V., Wood, D. A., Blewitt, D., Carouge, C. C., van Donkelaar, A., Jones, D. B. A., Murray, L. T. and Wang, Y.: Improved estimate of the policy-relevant background ozone in the United States using the GEOS-Chem global model with 1/2° × 2/3° horizontal resolution over North America, Atmos. Environ., 45(37), 6769–6776, doi:10.1016/j.atmosenv.2011.07.054, 2011.

Zhang, L., Jacob, D. J., Knipping, E. M., Kumar, N., Munger, J. W., Carouge, C. C., van Donkelaar, A., Wang, Y. X. and Chen, D.: Nitrogen deposition to the United States: distribution, sources, and processes, Atmos. Chem. Phys., 12(10), 4539–4554, doi:10.5194/acp-12-4539-2012, 2012.

Figure 1: Map of all participating NDACC stations. Detailed coordinates of each station are provided in Table 1.

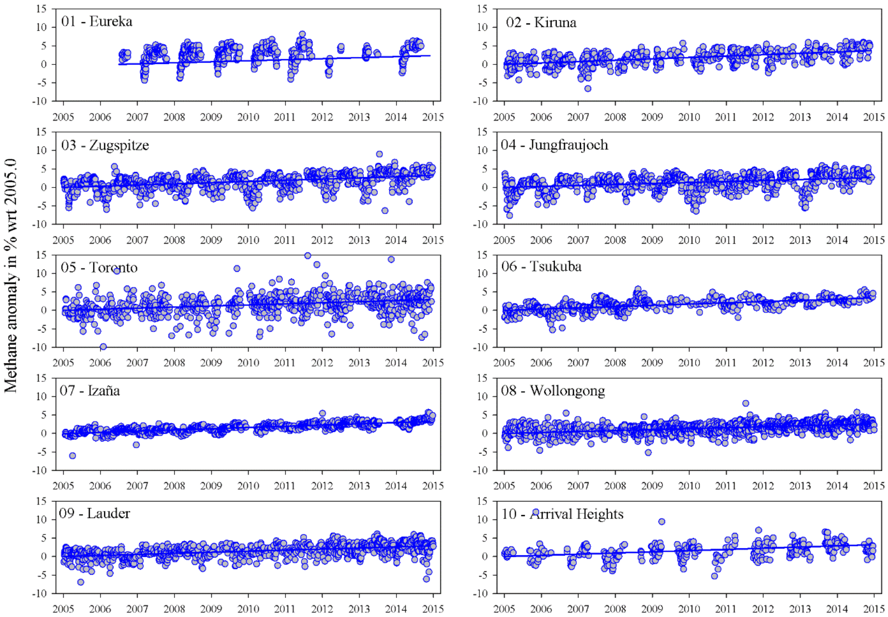

Figure 2: Daily mean methane anomaly with respect to 2005.0 or 2006.0 (in %) for 10 NDACC stations between 2005 and 2014. The blue line is the linear component of the bootstrap fit (see Sect. 3).

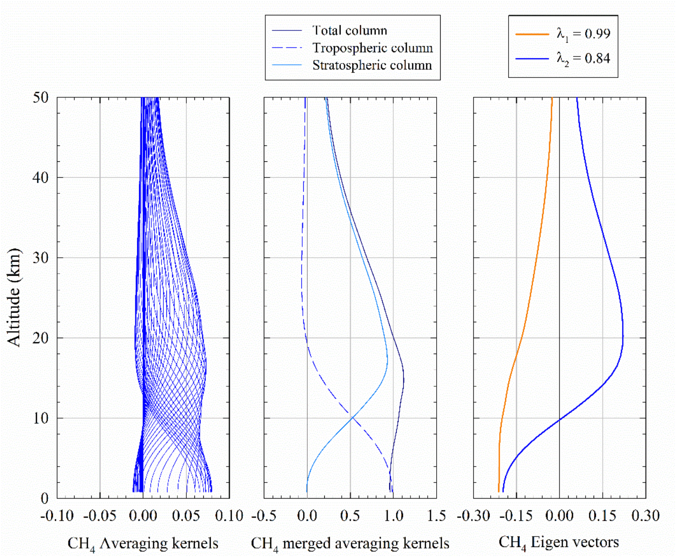

Figure 3: Typical ~~eigenvectors of a~~ NDACC methane retrieval. From left to right. First panel : typical individual (blue curves) CH_4 mixing ratio averaging kernels. Second panel : Merged (shades of blue curves) CH_4 mixing ratio averaging kernels. For merged-layer kernels, corresponding atmospheric column are specified in the legend box. Third panel : corresponding two first eigenvectors. Associated eigenvalues are given in the legend.

Mis en forme : Indice

Mis en forme : Indice

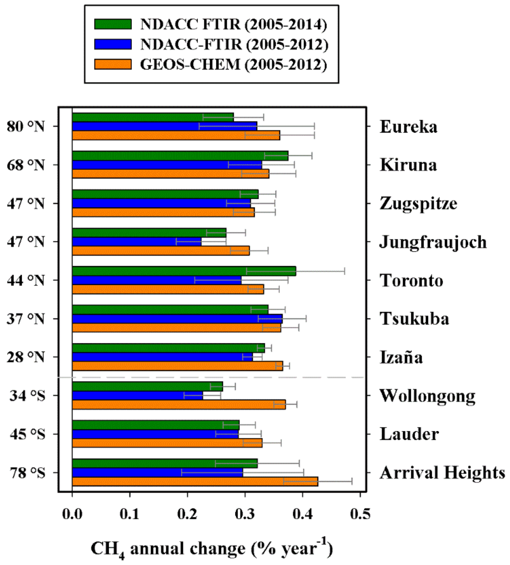

Figure 4: Methane total column mean annual change in % year^{-1} with respect to 2005.0 (2006.0 for Eureka), for the FTIR time series between 2005 and 2014 (in blue), the NDACC FTIR time series between 2005 and 2012 (in dark blue), and the GEOS-Chem simulation between 2005 and 2012 (in orange). Grey error bars represent 2-sigma uncertainty.

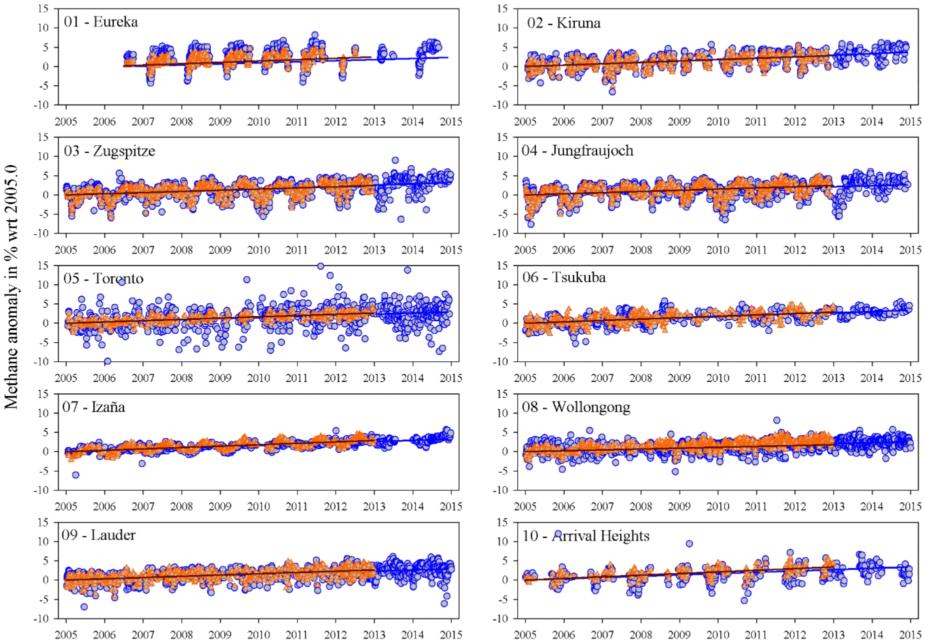

Figure 5: Daily mean CH$_4$ total columns~~methane~~ anomaly with respect to 2005.0 (in %) for ten NDACC stations between 2005 and 2014 for NDACC FTIR observations (in blue) and between 2005 and 2012 for the smoothed GEOS-Chem simulation (in orange) along with their respective linear component of the bootstrap fit in blue and brown.

Mis en forme : Indice

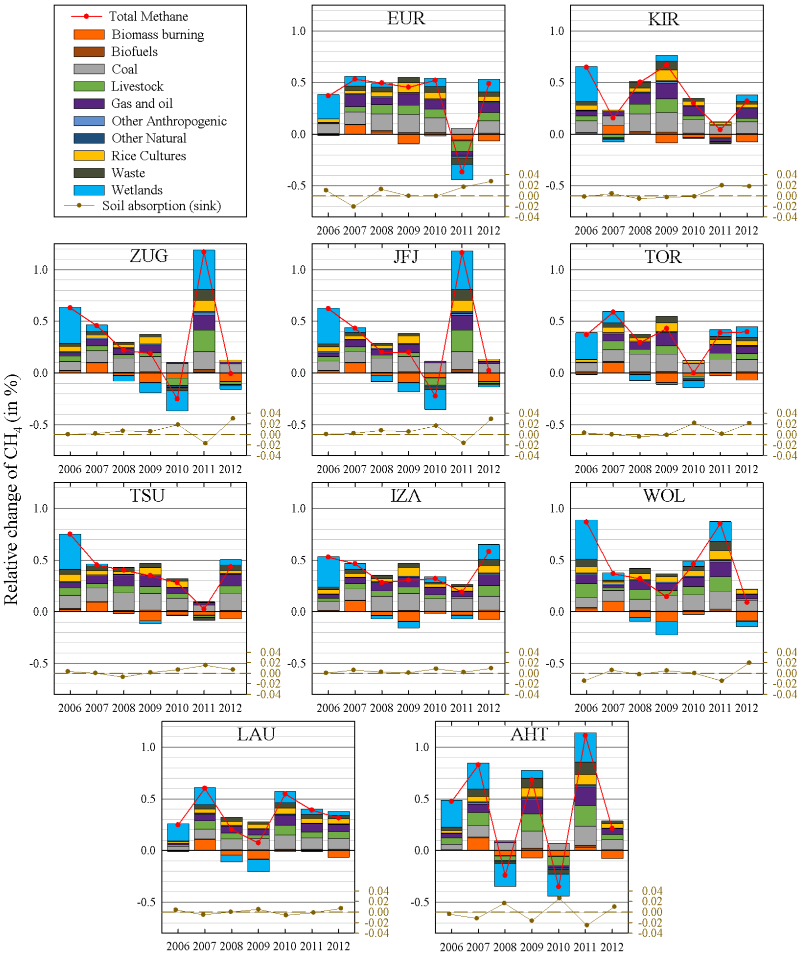

Figure 6: Year-to-year relative changes in CH_4 total columns due to each emission source (see color codes) for each station (see codes in Table 1) derived from GEOS-Chem. Brown circles represent the year-to-year relative changes of the methane sink due to soil absorption. Red circles illustrate the cumulative year-to-year methane change.

Station		Latitude (degrees north)	Longitude (degrees east)	Altitude (m)	# of days^a	Instrument
1	Eureka, EUR (CA)	80.05	- 86.42	610	^{b}619	Bruker IFS 125HR
2	Kiruna, KIR (SE)	67.84	20.39	420	649	Bruker IFS 120HR Bruker IFS 125HR
3	Zugspitze, ZUG (DE)	47.42	10.98	2 954	1114	Bruker IFS 125HR
4	Jungfraujoch, JFJ (CH)	46.55	7.98	3 580	1119	Bruker IFS 120HR
5	Toronto, TOR (CA)	43.66	- 79.4	174	964	ABB Bomem DA8
6	Tsukuba, TSU (JP)	36.05	140.12	31	640	Bruker IFS 120HR Bruker IFS 125HR
7	Izaña, IZA (ES)	28.29	- 16.48	2 370	990	Bruker IFS 120M Bruker IFS 125HR
8	Wollongong, WOL (AU)	- 34.41	150.88	31	1612	Bomem DA8 Bruker IFS 125HR
9	Lauder, LAU (NZ)	- 45.04	169.68	370	1017	Bruker IFS 120HR
10	Arrival heights, AHT (NZ)	- 77.83	166.65	200	^{c}341	Bruker IFS 120M

Table 1: Description of the participating stations. a. Number of days with CH$_4$ measurements available over the 2005-2014 time period. b. Measurements started in 2006 and no measurements between late October and late February due to polar night. c. No measurements between May and August due to polar night.

~~Station~~	**~~Retrieval code~~**	**~~Retrieval windows~~**	**~~Interfering gases~~**	**~~A priori & regularization~~**	**~~Linelist~~**
~~EUR~~	~~SFIT-4~~	~~3[a]~~	~~HDO, H_2O, CO_2, NO_2~~	~~[b] WACCM v6~~ ~~[c] Tikhonov L_1~~	~~[d] HIT-08~~
~~KIR~~	~~PROFFIT~~	~~6[e1]~~	~~H_2O, HDO, CO_2, O_3, N_2O, NO_2, HCl, OCS~~	~~WACCM v6~~ ~~Tikhonov L_1~~	~~[f] ad hoc CH_4~~ ~~HIT-08~~
~~ZUG~~	~~PROFFIT~~	~~3[a]~~	~~H_2O, HDO, CO_2, NO_2~~	~~WACCM v6~~ ~~Tikhonov L_1~~	~~[g] HIT-00~~
~~JFJ~~	~~SFIT-2 v3.94~~	~~6[e2]~~	~~H_2O, HDO, CO_2, O_3, NO_2, HCl~~	~~WACCM v6~~ ~~Tikhonov L_1~~	~~[f] ad hoc CH_4~~ ~~HIT-08~~
~~TOR~~	~~SFIT-4~~	~~3[a]~~	~~H_2O, HDO, CO_2, NO_2~~	~~WACCM v6~~ ~~Tikhonov L_1~~	~~HIT-08~~
~~TSU~~	~~SFIT-2 v3.94~~	~~3[a]~~	~~H_2O, HDO, CO_2, NO_2~~	~~[h] NIES Airplane~~ ~~Tikhonov L_1~~	~~HIT-00~~
~~IZA~~	~~PROFFIT~~	~~6[e1]~~	~~H_2O, HDO, CO_2, O_3, N_2O, NO_2, HCl, OCS~~	~~WACCM v6~~ ~~Tikhonov L_1~~	~~[f] ad hoc CH_4~~ ~~HIT-08~~
~~WOL~~	~~SFIT-2 v3.94~~	~~3[a]~~	~~H_2O, HDO, CO_2, NO_2~~	~~WACCM v5~~ ~~Tikhonov L_1~~	~~HIT-00~~
~~LAU~~	~~SFIT-2 v3.82~~	~~3[i]~~	~~HDO~~	~~[j] URAP at 44°S~~ ~~[k] OEM~~	~~HIT-00~~
~~AHT~~	~~SFIT-2 v3.82~~	~~3[i]~~	~~HDO~~	~~[l] ATMOS zonal mean~~ ~~OEM~~	~~HIT-00~~

~~Table 2: Retrieval parameters for each station. a. As detailed in Sussmann et al., (2011) b. Whole Atmosphere Community Climate Model, (Chang et al., 2008). c. Thikonov regularization as detailed in Tikhonov (1963). d. High-resolution transmission molecular absorption database, Hitran-2008 (Rothman et al., 2009). e. (e1) As detailed in or (e2) based on Sepúlveda et al. (2012). f. For all species, Hitran 2008 parameters are used. For methane, ad hoc adjustments performed by KIT, IMK-ASF are used (D. Dubravica, priv. comm., Dec 2012; see also Dubravica et al., 2013). g. Hitran-2000 including 2001 update release (Rothman et al., 2003). h. A priori profile for Tsukuba retrievals include monthly averaged profiles made from airplane measurements over Japan by the National Institute of Environmental Studies, Japan (NIES, http://www.nies.go.jp/index-e.html). i. As detailed in Rinsland et al., (2006). j. A priori profile for Lauder retrieval include annual mean of measurements from the Microwave Limb Sounder (MLS, https://mls.jpl.nasa.gov/) and the Halogen Occultation Experiment (HALOE, http://haloe.gats-inc.com/home/index.php) onboard the Upper Atmosphere Research Satellite (UARS, http://uars.gsfc.nasa.gov/) at 44°S in the framework of the UARS Reference Atmosphere Project (URAP, Grooß and Russell, 2005). k. Optimal Estimation Method based on the formalism of Rodgers (1990). l. A priori for Arrival Heights retrievals include zonal mean of measurements from the Atmospheric Trace Molecule Spectroscopy Experiment (ATMOS) Spacelab 3 over the 14-65 km altitude range (Gunson et al., 1996).~~

Mis en forme : Anglais (Royaume-Uni)

Mis en forme : Anglais (États-Unis)

Mis en forme : Anglais (Royaume-Uni)

Mis en forme : Anglais (États-Unis)

Mis en forme : Anglais (Royaume-Uni)

Mis en forme : Anglais (États-Unis)

	FTIR trend [2005-2014]		**FTIR trend [2005-2012]**		**FTIR Reference Column**	**Bias**	**GEOS-Chem trend [2005-2012]**		**GEOS-Chem Reference Column**
Unit	x 10^{16} molec cm^{-2} yr^{-1}	% yr^{-1}	x 10^{16} molec $cm^{-2}yr^{-1}$	% yr^{-1}	x 10^{19} molec cm^{-2}	%	x 10^{16} molec cm^{-2} yr^{-1}	% yr^{-1}	x 10^{19} molec cm^{-2}
EUR	9.54 ± 1.79	0.28 ± 0.05	10.81 ± 3.47	0.32 ± 0.10	3.41[a]	0.9 ± 2.9	12.35 ± 2.06	0.36 ± 0.06	3.46
KIR	13.26 ± 1.46	0.37 ± 0.04	11.7 ± 2.04	0.33 ± 0.06	3.54	-1.0 ± 1.5	12.04 ± 1.66	0.34 ± 0.05	3.53
ZUG	8.33 ± 0.80	0.32 ± 0.03	7.99 ± 1.09	0.31 ± 0.04	2.58	-0.7 ± 1.2	8.09 ± 0.93~~9.26~~	0.32 ± 0.04	2.56
JFJ	6.41 ± 0.81	0.27 ± 0.03	5.39 ± 1.04	0.22 ± 0.04	2.40	-0.8 ± 1.5	7.31 ± 0.78	0.31 ± 0.03	2.38
TOR	10.99 ± 3.03	0.29 ± 0.08	12.85 ± 3.76	0.34 ± 0.10	3.71	0.4 ± 5.9	12.45 ± 1.01	0.33 ± 0.03	3.75
TSU	12.99 ± 1.13	0.34 ± 0.03	13.90 ± 1.58	0.36 ± 0.04	3.82	-3.2 ± 3.1	13.36 ± 1.17	0.36 ± 0.03	3.69
IZA	9.56 ± 0.35	0.33 ± 0.01	8.96 ± 0.48	0.31 ± 0.02	2.87	-0.9 ± 1.3	10.34 ± 0.34	0.36 ± 0.01	2.83
WOL	9.62 ± 0.80	0.26 ± 0.02	8.33 ± 1.18	0.23 ± 0.03	3.69	0.6 ± 1.9	13.63 ± 0.74	0.37 ± 0.02	3.69
LAU	9.87 ± 0.95	0.29 ± 0.03	9.81 ± 1.34	0.29 ± 0.04	3.41	2.3 ± 1.7	11.46 ± 1.15	0.33 ± 0.03	3.48
AHT	10.53 ± 2.39	0.32 ± 0.07	9.70 ± 3.48	0.29 ± 0.11	3.28	4.8 ± 3.5	14.53 ± 2.02	0.43 ± 0.06	3.41
Mean	10.11 ± 2.03	0.31 ± 0.03	9.94 ± 2.50	0.30 ± 0.04	-		11.56 ± 2.35	0.35 ± 0.03	-

Table 2~~3~~ – Absolute (in molecules cm^{-2} $year^{-1}$) and relative (in % $year^{-1}$) annual change of methane total columns and its associated 2σ-uncertainties from FTIR observations and the GEOS-Chem methane simulation with respect to 2005.0 and to the reference column given in molecules cm^{-2} in the fifth and last columns of this table, respectively. The systematic bias between FTIR and GEOS-Chem for 2005-2012 and its associated 2σ-uncertainties are given in the sixth column. A positive bias can be translated into an overestimation of the GEOS-Chem simulation. a. Reference column for Eureka is for 2006.0 since no measurements are available before then. The bottom line of the table shows the average of the ten mean annual trends.

Appendix A - NDACC FTIR retrieval strategies

Mis en forme : Titre 1

Table A1 summarizes the retrieval parameters for methane for each station. FTIR measurements are analyzed as recommended either by Rinsland et al. (2006), Sussmann et al. (2011), or Sepúlveda et al. (2012). The spectral microwindows limits for the Eureka, Zugspitze, Toronto and Wollongong stations are based on Sussmann et al., (2011) and use the Hitran-2000 spectroscopic database including 2001 update release (Rothman et al., 2003) except for Toronto where Hitran 2008 was employed (Rothman et al., 2009). The microwindows used for the Kiruna, Jungfraujoch, Izaña observations are based on Sepulveda et al. (2012). For all interfering species, Hitran 2008 parameters are used. For methane, ad hoc adjustments performed by KIT, IMK-ASF are used (D. Dubravica, priv. comm., Dec 2012; see also Dubravica et al., 2013). Finally, the microwindows used for the Lauder and Arrival Heights observations are based on Rinsland et al. (2006). In order to better appraise the relatively low humidity rates at Jungfraujoch, a pre-fitting of the two microwindows (2611.60 - 2613.35 and 2941.65 - 2941.89) dedicated to water vapour and its isotopologue HDO is performed and used as a priori for the actual retrieval.

Mis en forme : Normal

A priori profiles for target and interfering molecules are based on the Whole Atmosphere Community Climate Model (version 5 or 6, WACCM, e.g. Chang et al., 2008) climatology, except for Tsukuba, Lauder and Arrival Heights. A priori profile for Tsukuba retrievals include monthly averaged profiles made from airplane measurements over Japan by the National Institute of Environmental Studies, Japan (NIES, http://www.nies.go.jp/index-e.html). A priori profile for Lauder retrieval include annual mean of measurements from the Microwave Limb Sounder (MLS, https://mls.jpl.nasa.gov/) and the Halogen Occultation Experiment (HALOE, http://haloe.gats-inc.com/home/index.php) onboard the Upper Atmosphere Research Satellite (UARS, http://uars.gsfc.nasa.gov/) at 44°S in the framework of the UARS Reference Atmosphere Project (URAP, Grooß and Russell, 2005). A priori for Arrival Heights retrievals include zonal mean of measurements from the Atmospheric Trace Molecule Spectroscopy Experiment (ATMOS) Spacelab 3 over the 14-65 km altitude range (Gunson et al., 1996). As mentioned in the Sect. 2.2.2. of this paper, a Tikhonov regularization (Tikhonov, 1963) is used and optimized in order to limit the value of the Degrees of Freedom For Signal (DOFS) to a value of approximately 2 (Sussmann et al., 2011) except for Lauder and Arrival Heights that uses an Optimal Estimation Method (OEM) based on the formalism of Rodgers (1990). Averaged DOFS value and associated 1-σ uncertainty are given in the last column of Table A1.

Station	Retrieval code	Retrieval windows (cm^{-1})	Interfering gases	A priori & regularization	Linelist	Averaged DOFS
EUR	SFIT-4	2613.7 – 2615.4	HDO CO_2	WACCM v6	HIT-08	2.31 ± 0.66
		2835.5 – 2835.8	HDO	Tikhonov L_1		
		2921.0 – 2921.6	HDO H_2O NO_2			
KIR	PROFFIT	2611.6 - 2613.35	HDO CO_2 N_2O (no CH_4)	WACCM v6	[f] ad hoc CH_4	2.35 ± 0.29
		2613.7 - 2615.4	HDO CO_2 O_3 N_2O	Tikhonov L_1	HIT-08	
		2835.55 - 2835.8	HDO O_3 N_2O			
		2903.82 - 2903.925	H_2O HDO O_3 NO_2 N_2O OCS HCl			
		2914.7 - 2915.15	H_2O HDO O_3 NO_2 OCS HCl			
		2941.51 - 2942.22	H_2O O_3 OCS (no CH_4)			
ZUG	PROFFIT	2613.7 - 2615.4	HDO CO_2	WACCM v6	[g] HIT-00	1.93 ± 0.32
		2835.5 - 2835.8	HDO	Tikhonov L_1		
		2921.0 - 2921.6	HDO H_2O NO_2			
JFJ	SFIT-2 v3.94	2611.60 - 2613.35	HDO CO_2 (no CH_4)	WACCM v6	[f] ad hoc CH_4	2.37 ± 0.46
		2613.7 - 2615.4	HDO CO_2 O_3	Tikhonov L_1	HIT-08	
		2835.55 - 2835.80	HDO O_3			
		2903.82 - 2903.925	H_2O HDO O_3 NO_2			
		2914.70 - 2915.15	H_2O HDO O_3 NO_2 HCl			
		2941.65 - 2941.89	H_2O O_3 (no CH_4)			
TOR	SFIT-4	2613.7 - 2615.4	HDO CO_2	WACCM v6	HIT-08	2.05 ± 0.69
		2835.5 - 2835.8	HDO	Tikhonov L_1		
		2921.0 - 2921.6	HDO H_2O NO_2			
TSU	SFIT-2 v3.94	2613.7 - 2615.4	HDO CO_2	[h] NIES Airplane	HIT-00	2.73 ± 0.18
		2835.5 - 2835.8	HDO	Tikhonov L_1		
		2921.0 - 2921.6	HDO H_2O NO_2			
IZA	PROFFIT	2611.6 - 2613.35	HDO CO_2 N_2O (no CH_4)	WACCM v6	[f] ad hoc CH_4	2.42 ± 0.28
		2613.7 - 2615.4	HDO CO_2 O_3 N_2O	Tikhonov L_1	HIT-08	
		2835.55 - 2835.8	HDO O_3 N_2O			
		2903.82 - 2903.925	H_2O HDO O_3 NO_2 N_2O OCS HCl			
		2914.7 - 2915.15	H_2O HDO O_3 NO_2 OCS HCl			
		2941.51 - 2942.22	H_2O O_3 OCS (no CH_4)			
WOL	SFIT-2 v3.94	2613.7 - 2615.4	HDO CO_2	WACCM v5	HIT-00	1.81 ± 0.28
		2835.5 - 2835.8	HDO	Tikhonov L_1		
		2921.0 - 2921.6	HDO H_2O NO_2			
LAU	SFIT-2 v3.82	2650.85 - 2651.25	HDO	[j] URAP at 44°S	HIT-00	2.96 ± 0.73
		2666.95 - 2667.35	HDO	[k] OEM		
		2673.90 - 2674.41	HDO			
AHT	SFIT-2 v3.82	2650.85 - 2651.25	HDO	[l] ATMOS zonal mean	HIT-00	3.54 ± 0.76
		2666.95 - 2667.35	HDO			

2673.90 - 2674.41	HDO	OEM

Table A1: Retrieval parameters for each station.

Mis en forme : Légende

Appendix B – Top three contributors to the methane increase as simulated by GEOS-Chem

Table B~~A~~1 illustrates the first three contributors to the annual methane change and their year-to-year changes for each site along with the cumulative relative increase for the whole 2005-2012 time period. The GEOS-Chem tracers are coded as follows: biomass burning (bb), biofuels (bf), coal (co), livestock (li), gas and oil (ga), other anthropogenic sources (oa), other natural sources (on), rice cultivation (ri), waste management (wa), wetlands (wl).

Station	**%**	**2005 → 2006**	**2006 → 2007**	**2007 → 2008**	**2008 → 2009**	**2009 → 2010**	**2010 → 2011**	**2011 → 2012**	**2005 → 2012**
EUR	tracers	wl 0.23	co 0.12	co 0.16	co 0.17	co 0.14	wl -0.15	wl 0.12	co 0.87
		co 0.10	ga 0.12	li 0.09	ga 0.11	ga 0.11	li -0.11	co 0.12	ga 0.46
		ri 0.03	bb 0.09	ga 0.07	ri 0.09	ri 0.09	wa -0.06	ga 0.09	wl 0.42
	total	**0.37**	**0.53**	**0.49**	**0.45**	**0.52**	**-0.37**	**0.49**	**2.49**
KIR	tracers	wl 0.34	co 0.34	co 0.17	co 0.19	co 0.13	co 0.09	co 0.11	co 0.98
		co 0.11	bb 0.11	ga 0.10	ga 0.15	ga 0.09	bb -0.03	ga 0.10	ga 0.51
		ga 0.05	ga 0.05	li 0.09	ri 0.17	ri 0.04	ga -0.03	wl 0.06	wl 0.44
	total	**0.65**	**0.15**	**0.50**	**0.67**	**0.30**	**0.04**	**0.32**	**2.63**
ZUG	tracers	wl 0.35	co 0.11	co 0.14	co 0.15	wl -0.20	wl 0.38	co 0.09	co 0.83
		co 0.09	bb 0.10	ga 0.06	ga 0.08	li -0.07	li 0.21	bb -0.08	wl 0.42
		ri 0.05	ga 0.07	li 0.03	ri 0.07	bb -0.05	co 0.17	*sa 0.03*	ga 0.41
	total	**0.63**	**0.46**	**0.22**	**0.19**	**-0.25**	**1.17**	**-0.01**	**2.40**
JFJ	tracers	wl 0.35	co 0.11	co 0.14	co 0.15	wl -0.19	wl 0.38	wl 0.38	co 0.09
		co 0.11	bb 0.10	ga 0.06	ga 0.08	li -0.06	li 0.21	li 0.21	bb -0.08
		ri 0.05	ga 0.06	li 0.03	ri 0.07	bb -0.05	co 0.17	co 0.17	*sa -0.03*
	total	**0.62**	**0.43**	**0.20**	**0.20**	**-0.22**	**1.16**	**1.16**	**2.41**
TOR	tracers	wl 0.26	co 0.12	co 0.17	co 0.17	co 0.09	co 0.13	co 0.12	co 0.87
		co 0.09	wl 0.11	ga 0.07	ga 0.17	wl -0.06	ga 0.08	wl 0.10	ga 0.43
		ri 0.03	bb 0.10	li 0.05	ri 0.08	bb -0.03	wl 0.06	ga 0.07	wl 0.40
	total	**0.37**	**0.59**	**0.29**	**0.43**	**0.00**	**0.39**	**0.40**	**2.46**
TSU	tracers	wl 0.34	co 0.13	co 0.17	co 0.16	co 0.12	co 0.06	co 0.16	co 0.94
		co 0.13	bb 0.09	ga 0.10	ga 0.10	ri 0.06	ga 0.02	ga 0.11	ga 0.52
		li 0.07	ga 0.07	li 0.07	ri 0.07	ga 0.05	bb -0.03	li 0.08	wl 0.39
	total	**0.75**	**0.45**	**0.40**	**0.35**	**0.28**	**0.03**	**0.43**	**2.69**
IZA	tracers	wl 0.30	co 0.11	co 0.14	co 0.16	co 0.12	co 0.12	wl 0.15	co 0.87
		co 0.09	bb 0.11	ga 0.08	ga 0.10	ga 0.07	ga 0.07	co 0.13	ga 0.49
		ri 0.04	wl 0.06	li 0.05	ri 0.08	wl 0.06	ri 0.04	li 0.11	wl 0.15
	total	**0.53**	**0.46**	**0.28**	**0.31**	**0.32**	**0.19**	**0.58**	**2.67**
WOL	tracers	wl 0.38	bb 0.10	co 0.11	co 0.15	co 0.15	wl 0.19	co 0.10	co 0.78
		li 0.14	co 0.10	li 0.09	ga 0.07	ga 0.09	co 0.17	bb -0.09	li 0.52
		co 0.09	wl 0.07	ga 0.09	ri 0.06	li 0.08	li 0.15	ga 0.04	ga 0.51
	total	**0.87**	**0.37**	**0.32**	**0.14**	**0.46**	**0.85**	**0.09**	**3.01**
LAU	tracers	wl 0.17	wl 0.17	co 0.10	co 0.11	co 0.13	co 0.11	co 0.10	ca 0.70
		co 0.04	bb 0.11	ga 0.06	ga 0.06	wl 0.11	ga 0.08	ga 0.07	ga 0.43
		ri 0.02	co 0.09	li 0.06	wl -0.12	li 0.10	li 0.05	li 0.07	li 0.41
	total	**0.25**	**0.60**	**0.20**	**0.07**	**0.55**	**0.39**	**0.31**	**2.37**
AHT	tracers	wl 0.26	wl 0.25	wl -0.22	li 0.17	wl -0.21	wl 0.29	co 0.10	co 0.75
		li 0.06	li 0.13	bb -0.05	co 0.17	li -0.09	li 0.20	ga 0.06	ga 0.48
		co 0.05	bb 0.12	co 0.07	ga 0.14	co 0.07	co 0.18	li 0.04	li 0.47
	total	**0.47**	**0.83**	**-0.24**	**0.68**	**-0.35**	**1.11**	**0.21**	**2.71**

Table B~~A~~1. Top three simulated tracers contributing the most to the methane changes, per year and per site, in %.